VEGETATION DYNAMICS AND SEA-LEVEL CHANGES IN THE UPPER GULF OF THAILAND

Miss Dissaya Sukaudom

A Thesis Submitted in Partial Fulfillment of the Requirements
for the Degree of Master of Science in Earth Sciences
Department of Geology
Faculty Of Science
Chulalongkorn University
Academic Year 2023

พลวัตของพืชพรรณและการเปลี่ยนแปลงของระดับน้ำทะเลบริเวณอ่าวไทยตอนบน

น.ส.ดิษยา สุขอุดม

วิทยานิพนธ์นี้เป็นส่วนหนึ่งของการศึกษาตามหลักสูตรปริญญาวิทยาศาสตรมหาบัณฑิต

สาขาวิชาโลกศาสตร์ ภาควิชาธรณีวิทยา

คณะวิทยาศาสตร์ จุฬาลงกรณ์มหาวิทยาลัย

ปีการศึกษา 2566

Thesis Title	VEGETATION DYNAMICS AND SEA-LEVEL CHANGES IN THE UPPER GULF OF THAILAND
By	Miss Dissaya Sukaudom
Field of Study	Earth Sciences
Thesis Advisor	Assistant Professor AKKANEEWUT JIRAPINYAKUL, Ph.D.
Thesis Co Advisor	Assistant Professor Paramita Punwong, Ph.D.

Accepted by the FACULTY OF SCIENCE, Chulalongkorn University in Partial Fulfillment of the Requirement for the Master of Science

--- Dean of the FACULTY OF SCIENCE

(Professor PRANUT POTIYARAJ, Ph.D.)

THESIS COMMITTEE

--- Chairman

(Professor SRILERT CHOTPANTARAT, Ph.D.)

--- Thesis Advisor

(Assistant Professor AKKANEEWUT JIRAPINYAKUL, Ph.D.)

--- Thesis Co-Advisor

(Assistant Professor Paramita Punwong, Ph.D.)

--- Examiner

(Professor SANTI PAILOPLEE, Ph.D.)

--- External Examiner

(Trongjai Hutangkura, Ph.D.)

ดิษยา สุขอุดม : พลวัตของพืชพรรณและการเปลี่ยนแปลงของระดับน้ำทะเลบริเวณอ่าวไทยตอนบน. (VEGETATION DYNAMICS AND SEA-LEVEL CHANGES IN THE UPPER GULF OF THAILAND) อ.ที่ปรึกษาหลัก : ผศ. ดร.อัคนีวุธ จิรภิญญากุล, อ.ที่ปรึกษาร่วม : ผศ. ดร.ปรมิตา พันธ์วงศ์

การเปลี่ยนแปลงสภาพภูมิอากาศมีบทบาทสำคัญต่อการรุกเข้าและถดถอยของระดับน้ำทะเลซึ่งสามารถนำไปสู่วิวัฒนาการของแนวชายฝั่ง จากการที่จังหวัดสมุทรสาครตั้งอยู่ในเขตชายฝั่งทะเลในพื้นที่อ่าวไทยตอนบน ดังนั้นการศึกษาการเปลี่ยนแปลงของระดับน้ำทะเลในอดีตบริเวณนี้จึงสามารถเพิ่มความเข้าใจเกี่ยวกับพลวัตของตะกอนและพัฒนาการของแนวชายฝั่งทะเลได้ จากพื้นที่ศึกษาสามารถแบ่งลำดับตะกอนออกเป็น 9 หน่วยจากความลึก 25.5-7.2 เมตรจากผิวดิน การวิเคราะห์ค่าที่หายไปจากการเผา อัตราส่วนไทเทเนียมต่อแคลเซียม อัตราส่วนเซอร์โคเนียมต่อรูบิเดียม ขนาดของตะกอน และเรณูวิทยา ถูกนำมาตีความร่วมกับการหาอายุของเรดิโอคาร์บอน โดยสามารถจำลองสภาพแวดล้อมในอดีตออกเป็น 2 ช่วง ได้แก่ ช่วงยุคไพลสโตซีนตอนปลาย (26,500-22,700 ปีมาแล้ว) โดยที่ช่วงเวลานี้พื้นที่ของสมุทรสาครอยู่เหนือระดับน้ำทะเล และช่วงยุคโฮโลซีนตอนกลางถึงตอนปลาย (5,400-1,100 ปีมาแล้ว) สภาพแวดล้อมในพื้นที่ศึกษามีลักษณะเป็นป่าชายเลนเนื่องจากเพิ่มขึ้นของระดับน้ำทะเลในช่วง 5,400-4,400 ปีมาแล้ว หลังจากนั้นระดับน้ำทะเลลดลงทำให้สภาพแวดล้อมเปลี่ยนจากป่าชายเลนเป็นแบบหลังป่าชายเลนในช่วง 4,400-4,200 ปีมาแล้ว และพื้นที่ชุ่มน้ำในช่วง 4,200-2,300 ปีมาแล้ว ก่อนที่ระยะต่อมาระดับน้ำทะเลจะเพิ่มสูงขึ้นอีกครั้งทำให้สภาพแวดล้อมในพื้นที่สมุทรสาครเปลี่ยนเป็นพื้นที่น้ำกร่อยในช่วง 2,300-1,100 ปีมาแล้ว สำหรับงานวิจัยในอนาคต ควรมีการบูรณาการร่วมกันของระดับที่ได้จากเครื่องวัดระดับอัตโนมัติและระบบบอกตำแหน่งโดยใช้พิกัดอ้างอิงเพื่อลดความคลาดเคลื่อนของข้อมูลและระดับที่ได้จะมีความน่าเชื่อถือมากขึ้น

สาขาวิชา	โลกศาสตร์	ลายมือชื่อนิสิต ....
ปีการศึกษา	2566	ลายมือชื่อ อ.ที่ปรึกษาหลัก ....
		ลายมือชื่อ อ.ที่ปรึกษาร่วม ....

6470095223 : MAJOR EARTH SCIENCES
KEYWORD:

Dissaya Sukaudom : VEGETATION DYNAMICS AND SEA-LEVEL CHANGES IN THE UPPER GULF OF THAILAND. Advisor: Asst. Prof. AKKANEEWUT JIRAPINYAKUL, Ph.D. Co-advisor: Asst. Prof. Paramita Punwong, Ph.D.

Climate change plays a role in sea level fluctuation, either transgression or regression leads to coastline evolution. Samut Sakhon province is located on the coast in the upper Gulf of Thailand therefore past sea-level studies in this area can contribute information to a better understanding of sediment dynamics and assess future coastline development. The study site provides sedimentary sequences consisting of 9 sediment units from 25.5-7.2 m. DBS, results of LOI, Ti/Ca, and Zr/Rb ratio, grain size, and pollen analysis were interpreted together with radiocarbon dating to reconstruct past environments in the study site. The past environment in Samut Sakhon site can divided into two parts in the late Pleistocene (26.5-22.7 cal ka BP), Samut Sakhon was temporal exposure during dry conditions, and in the mid/late Holocene (5.4-1.1 cal ka BP), mangrove forests grew due to sea level transgression at 5.4-4.4 cal ka BP before being transferred into the back-mangrove forest at 4.4-4.2 cal ka BP and wetland during sea level regression at 4.2-2.3 cal ka BP, respectively. Samut Sakhon site was likely to be a brackish area thereafter at 2.3-1.1 cal ka BP. To improve the level accuracy and decrease data discrepancies, autonomous level monitoring, and differential global positioning systems should be used in combination with future research.

Field of Study:	Earth Sciences	Student's Signature ....
Academic Year:	2023	Advisor's Signature ....
		Co-advisor's Signature ....

ACKNOWLEDGEMENTS

I would like to express my sincere thanks to my thesis advisor, Assistant Professor Akkaneewut Jirapinyakul, Ph.D. for his invaluable help and constant encouragement throughout the course of this research. I am most grateful for his advice and guidelines not only research methodologies but also many other methodologies in life. I would not have achieved this far without all the support that I have always received from him.

Moreover, I am grateful for the advice and knowledge of palynological study and laboratory techniques that I received from my co-advisor, Assistant Professor Paramita Punwong, Ph.D. from the Faculty of Environment and Resource Studies, Mahidol University.

Finally, I am most grateful for the support from my family and friends who assisted me throughout the period of this research.

Dissaya Sukaudom

TABLE OF CONTENTS

LIST OF TABLES

LIST OF FIGURES

CHAPTER 1
INTRODUCTION

1.1 Background

Climate change plays a role in sea level fluctuation. Either transgression or regression may subsequently change coastal sediment dynamics, leading to coastline development (Surakiatchai et al., 2018; Zhang et al., 2022; Zhang et al., 2023). Furthermore, coastal erosion rates and saltwater intrusion caused by rising sea levels alter the vegetation dynamics along the coastline (Choowong et al., 2004; Surakiatchai et al., 2018). These influences of sea level changes will dramatically impact the livelihoods, including humans, animals, and plants, along the coastline. The study of past sea level changes can contribute information to a better understanding of sediment dynamics and assess future coastline development for sustainability management in the coastal area.

The Gulf of Thailand has been considered to be a crucial area for sea level change studies (Hanebuth et al., 2000; Horton et al., 2005; Chabangborn et al., 2020). It is located in a tropical climate and is unaffected by isostatic movement. Moreover, the evidence of tectonic activities is indeterminable in the Gulf of Thailand (Horton et al., 2005; Oliver & Terry, 2019). Therefore, the sea level changes in the Gulf of Thailand are possibly caused by the eustatic changes (Horton et al., 2005).

Samut Sakhon province is located on the coast in the lower central plain that considered to be a potential area for hydrocarbon accumulation, 5 km north of the upper Gulf of Thailand (Sinsakul, 2000). Moreover, the neighborhood area at the coast in Samut Sakhon is mostly shrimp farms and open pits where topsoil was dug out and shows a clear sediment profile that is suitable for paleoenvironmental study.

The sea level changes along the Gulf of Thailand have been reconstructed by various proxies, i.e., the radiocarbon dating of peat layer or shell attached to sea notch (Somboon, 1990; Tjia, 1996; Hutangkura, 2014; Surakiatchai et al., 2018), geomorphology (Bird et al., 2007; Tamura et al., 2009; Li et al., 2012; Surakiatchai et al., 2018), sedimentology, and palynology (Nudnara, 2019; Chabangborn et al., 2020; Sainakum et al., 2021). Although many studies have been done to date, more information is necessitated to constrain the uncertainty of environmental reconstruction.

1.2 Research objectives

To investigate the temporal variabilities of sea level, vegetation dynamics, and coastal evolution in the upper Gulf of Thailand.

1.3 Scope of the study

This study focuses on investigating vegetation dynamics associated with the sea level changes at an open pit in Samut Sakorn province (13° 32.145'N to13° 32.155'N and 100° 21.684'E to 100° 21.725'E). The open pit covering an area of approximately 0.42 km^2, located approximately 5 km north of the upper Gulf of Thailand. Sediment samples were collected from the bottom to the top of the open pit (25.48-7.20 mDBS). A total of 145 samples were further studied at the Department of Geology, Faculty of Science, Chulalongkorn University. For laboratory analysis, 145 samples from consecutive 10 cm were used for Loss on ignition (LOI) and X-ray Fluorescence Spectroscopy (XRF), 11 samples were used for radiocarbon dating (C14), 60 samples were used for pollen analysis, and 73 samples were used for grain size analysis.

CHAPTER 2
LITERATURE REVIEW

2.1 Mangrove response

Mangrove environments are dominant assemblages of trees and shrubs that developed special physiological and morphological adaptations in saline tidal wetlands fringing the sheltered tropical shores (Santisuk, 1983; Ellison, 2008; Li et al., 2012; Englong et al., 2019). The development of a mangrove community depends on several environmental factors, including tidal flooding, maximum wave height or inundation, soil type, and salinity (Santisuk, 1983; Li et al., 2012).

Watson (1928) classified the total water level that occurs on normally dry ground as a result of the storm tide as tidal inundation into 5 classes associated with the distribution of mangrove trees and shrubs in Malaya (Table 1).

Table 1 Tidal inundation class from Watson (1928)

Class	Flood type	Frequency (times per month)
1	All high tides	56 - 62
2	Medium high tides	45 - 59
3	Normal high tides	20 - 45
4	Spring tides	2 - 20
5	Abnormal of equinoctial tides	0 - 2

According to Watson's inundation classes, mangroves can be divided into 2 subdivisions, swampy mangroves or mangroves and back mangroves from inundation classes 1-3 and 4-5, respectively (Watson, 1928; Santisuk, 1983). Swampy mangroves or mangroves are normally submerged and covered by sea water during high tide, while back mangroves are only submerged during very high tides (Santisuk, 1983).

Santisuk (1983) developed Watson's inundation classes associated with mangrove distribution in Thailand (Table 2).

Table 2 Mangrove tree and shrub distribution in Thailand based on Watson's (1928)

Scientific name	Family	Ecological appearance	
		Mangroves	Back mangroves
Acrostichum aureum	Pteridaceae		✓
Acrostichum speciosum	Pteridaceae		✓
Avicennia alba	Avicenniaceae	✓	
Avicennia marina	Avicenniaceae	✓	
Avicennia officinalis	Avicenniaceae	✓	
Baringtonia asiatica	Baringtoniaceae		✓
Baringtonia racemosa	Baringtoniaceae		✓
Brownlowia tersa	Tiliaceae		✓
Bruguiera cylindrica	Rhizophoraceae	✓	
Bruguiera gymnorrhiza	Rhizophoraceae	✓	
Bruguiera parviflora	Rhizophoraceae	✓	
Bruguiera sexangula	Rhizophoraceae		✓
Ceriops decandra	Rhizophoraceae	✓	
Ceriops tagal	Rhizophoraceae	✓	
Lumnitzera littorea	Combretaceae		✓
Lumnitzera racemosa	Combretaceae		✓
Melaleuca leucadendron	Myrtaceae		✓
Nypa fructicans	Arecaeae		✓
Oncosperma tigillaria	Arecaeae		✓

Pluchea indica	Asteraceae		✓
Rhizophora apiculata	Rhizophoraceae	✓	
Rhizophora mucronata	Rhizophoraceae	✓	
Sonneratia alba	Sonneratiaceae	✓	
Sonneratia caseolaris	Sonneratiaceae		✓
Sonneratia griffithii	Sonneratiaceae		✓
Sonneratia ovata	Sonneratiaceae		✓
Suaeda maritima	Chenopodiaceae		✓
Xylocarpus gangeticus	Miliaceae		✓
Xylocarpus granatum	Miliaceae		✓
Xylocarpus moluccensis	Miliaceae		✓

Mangrove trees and shrubs can be interpreted by palynology which is the study of pollen and spores of plants. Pollen and spores contain sporopollenin which is a special structure of the durable outer (exine) walls of spores and pollen grains that can protect itself from external factors such as temperature, acidity, and alkalinity. This property together with their high productivity made pollen and spores are well preserved in sediment and a suitable tool for the reconstruction of the past environments (Punwong, 2007).

2.2 History of sea level changes in the Gulf of Thailand

Sea level changes have been considered to be possibly caused by isostatic rebound, tectonic adjustment, and eustatic changes. Since the Gulf of Thailand is in a tropical climate and far from ice sheet margins (Long et al., 2001), it is not impacted by the isostatic adjustment (Horton et al., 2005; Zhang et al., 2022). Moreover, the evidence of tectonic movement is indeterminable in the Gulf of Thailand. Therefore, it has been considered to be stable, and tectonic movement can be neglectable (Tjia, 1996; Horton et al., 2005; Jirapinyakul et al., 2023). Consequently, the Gulf of Thailand is a crucial area for eustatic changes (Sainakum et al., 2021). The sea level changes along the Gulf of Thailand and surrounding areas have been reconstructed based on various methods, i.e., geomorphology (Choowong, 2002; Dusitapirom et al., 2008; Surakiatchai et al., 2018; Oliver & Terry, 2019), Diatom (Zhang et al., 2023), radiocarbon dating of peat layers (Hesp et al., 1998; Bird et al., 2007), X-Ray Fluorescence, sedimentology and palynology (Somboon, 1988, 1990; Somboon & Thiramongkol, 1992; Nudnara, 2019; Chabangborn et al., 2020).

The global sea level was approximately 120 meters below the present mean sea level (MSL) during the Last Glacial Maximum (23.0 to 19.0 cal ka BP) when glaciers and ice sheets in the high latitudes reached their maximum (Hanebuth et al., 2000b; Tanabe et al., 2003; Zong, 2013) (Figures 1 and 2). The sea level low stand can be explained by the transformation of ocean water to deposit on the continental ice sheets caused by the changing Earth's orbit (Bowen, 2009). The sea level in the Gulf of Thailand was also lowering, exposing the Sunda shelf, connecting the Southeast Asian mainland and Indonesian archipelagos (Hanebuth et al., 2000a; Bird et al., 2007). The exposure of Sundaland was a land bridge for the migration of animals and humans to the Indonesian archipelagos and Australia (Zhang et al., 2022).

Sea levels rapidly increased during the early Holocene (approximately 11.7 to 8.2 ka BP) (Geyh et al., 1979; Hanebuth et al., 2000a; Horton et al., 2005; Hutangkura, 2014). Reconstruction of the sea level based on pollen and sediments from the Malay-Thai peninsula reveals the sea level rise at 9,700 cal years BP and reaches its highstand at 4.8 –4.4 cal ka BP (Horton et al., 2005). The reconstructed transgression in the Malay-Thai peninsula has a slight lead or lag in time regarding the other studies from the vicinity areas, e.g., records of *Sonneratia alba* and *Sonneratia caseolaris*, mangrove pollen taxa, that appeared in the sediment at 8.3 ka cal year BP, Mekong River Delta, Cambodia (Li et al., 2012), and radiocarbon dating of peat layer in Singapore (Bird et al., 2007). Pollen records of Chao Phraya delta suggest a submerge most of the Chao Phraya delta up to the north of Ayutthaya, Thailand, at 7.3–6.5 ka BP (Somboon & Thiramongkol, 1992) (Figure 3). In addition, the recent studies based on multi-proxies obtained from Thale Noi, Thailand, suggested that the sea level fluctuation at 8.2 ka during the early Holocene (Chabangborn et al., 2020). However, all these studies agree on the rapid rise of sea levels during the early Holocene.

Several studies suggest that the sea level reached its high stand of c. 2-4 m during the mid-Holocene (8.0-4.0 cal ka BP) (Somboon & Thiramongkol, 1992; Horton et al., 2005; Bird et al., 2010; Li et al., 2012; Hutangkura, 2014; Surakiatchai et al., 2018) (Figure 3, 4 and 5). However, the timing of the mid-Holocene high stand has been under-debated. Hutangkura (2014), for example, reconstructed the sea level in Chao Phraya Plain, Thailand, regarding pollen records and suggested the highstand at 8.4 cal ka BP. However, the dating of the peat layer by Somboon and Thiramongkol (1992) indicated a highstand of around 7.3–6.0 ka BP, which is consistent with those from Singapore by Tjia (1996) and Bird et al. (2010). Meanwhile, Horton et al. (2005) suggest that the sea level high stand was at 4.8–4.4 cal ka BP. The discrepancies can be explained by the lack of high-resolution radiocarbon dating (Chabangborn et al., 2020). Alternatively, the inconsistencies are possibly caused by the different responding times of proxies on the environmental shift (Wohlfarth et al., 2012). Otherwise, the sea levels in the Gulf of Thailand were not straightforward, with either gradual rise or fall, but they are punctuated by several time intervals of abrupt changes.

In the late Holocene, the sea level has been gradually fallen from the mid-Holocene high stand (Horton et al., 2005; Zong, 2013; Surakiatchai et al., 2018) (Figure 5). However, the record of the Malay-Thai Peninsular (Tjia, 1996) and evidence of the coastal area of Thailand (Sinsakul, 1992) suggest a fluctuating sea level after mid

Holocene high stand at 5.0-6.0 ka BP (Figure 6). Moreover, a recent study of pollen records from Sam Roi Yot wetland on the west coast of the Gulf of Thailand also suggests sea level fluctuation after high stand, significant regression occurred at 2.9 and 1.8-1.4 cal ka BP, sea level again raised at 1.4-1.0 cal ka BP before declining hereafter (Jirapinyakul et al., 2023). These arguments of the Late Holocene sea level are still under debate therefore further studies in detail are needed.

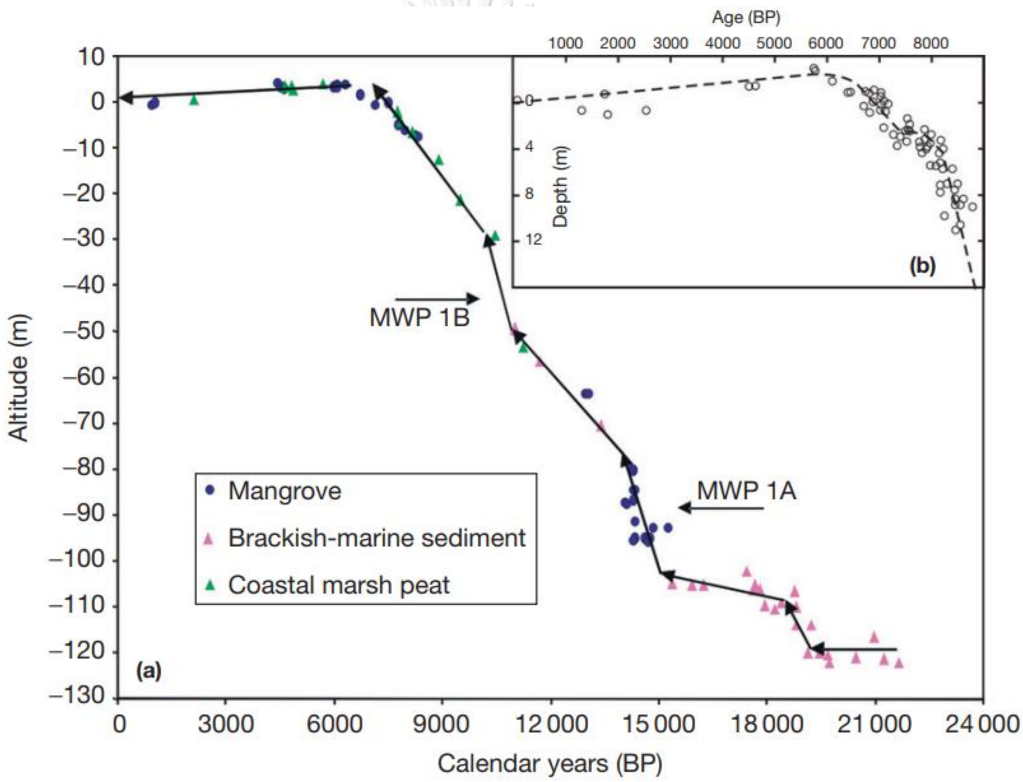

Figure 1 A relative sea-level curve (a) based on sea-level index points compiled from the Bonaparte Gulf, north Australia (Yokoyama et al., 2000), the Sunda Shelf (Hanebuth et al., 2000), and the Strait of Malacca (Geyh et al., 1979). A new record (b) from Singapore (Bird et al., 2010) shows that sea-level rise slowed down around 8000 years BP and accelerated around 7500 years BP (Zong, 2013).

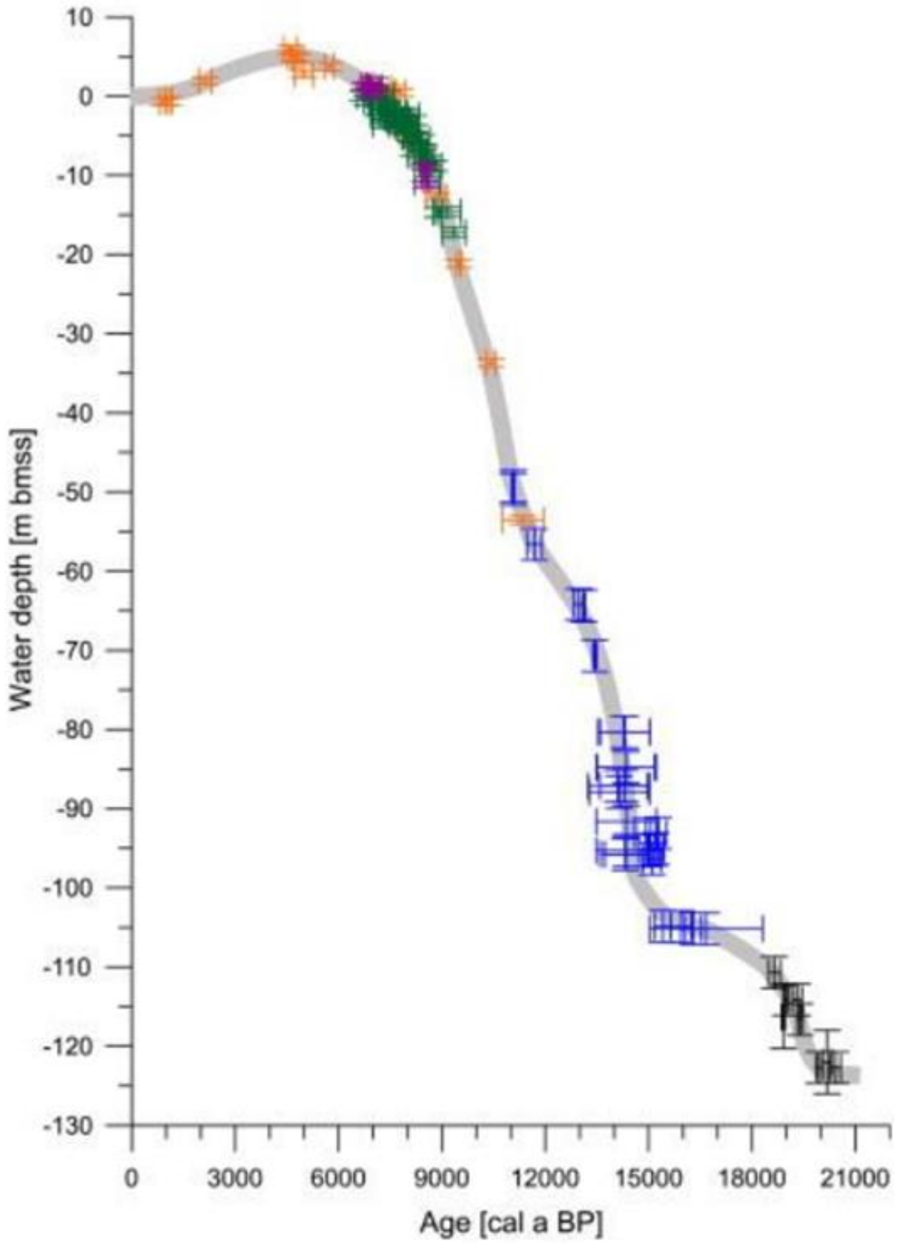

Figure 2 Reconstruction of sea level history for the past 21 ka showing all data recently available from the Sunda core region. Data compiled from Geyh et al. (1979) (orange; Strait of Malacca), Hesp et al. (1998) (purple; Singapore), and Hanebuth et al. (2009) (black; Sunda Shelf) (Hanebuth et al., 2011).

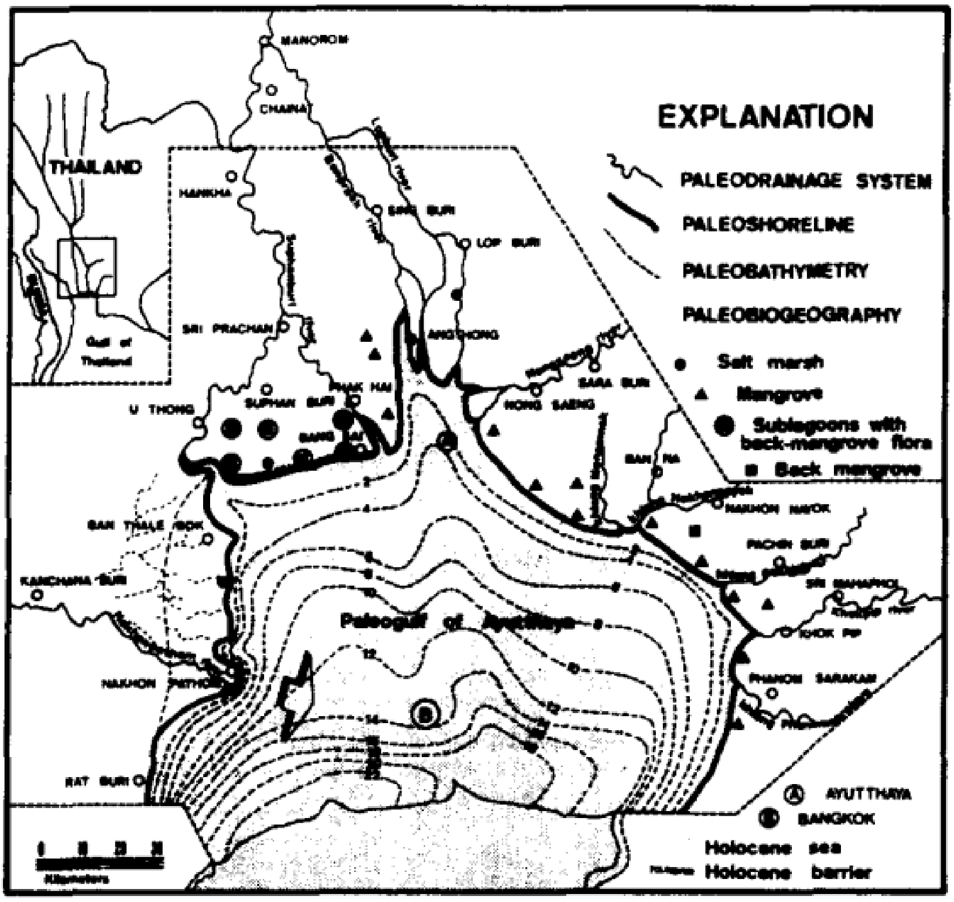

Figure 3 Paleogeographic map shows the old coastal in the Chao Phraya delta, Thailand (Somboon & Thiramongkol, 1992).

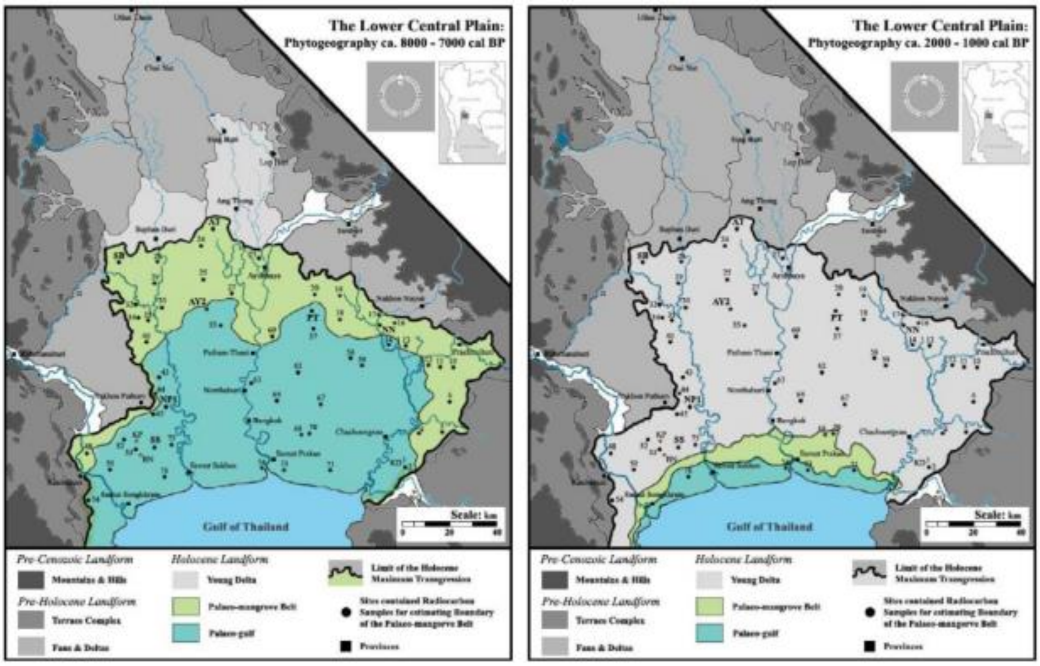

Figure 4 Paleogeography map at 8.0-7.0 cal ka BP and at 2.0-1.0 cal ka BP of the Lower Central Plain in Thailand (Hutangkura, 2012).

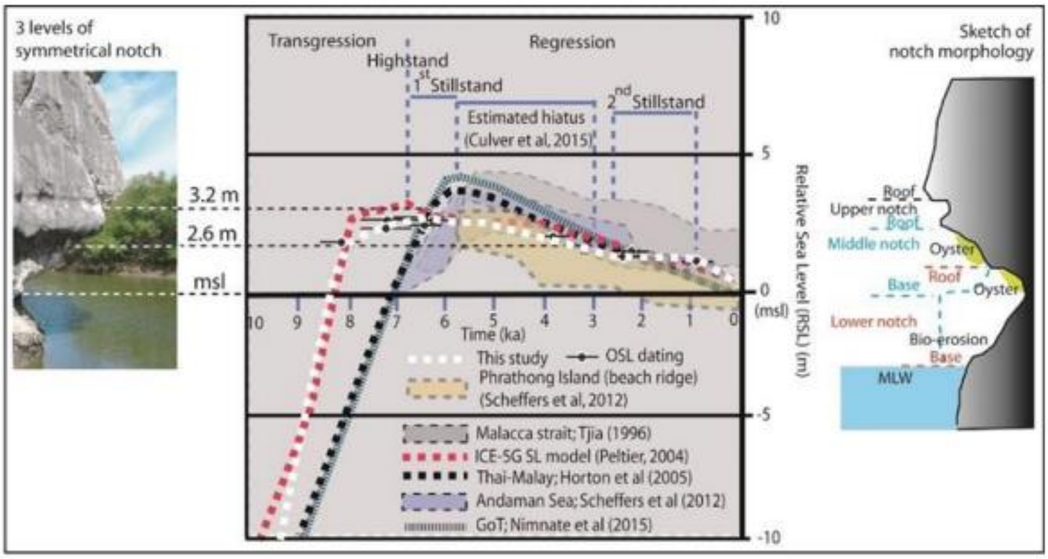

Figure 5 Comparison of sea-level curves from Southeast Asia and the South China Sea with the levels of sea notch (left), the white dash line show the proposed sea-level curve from Sam Roi Yot National Park, Thailand (Surakiatchai et al., 2018).

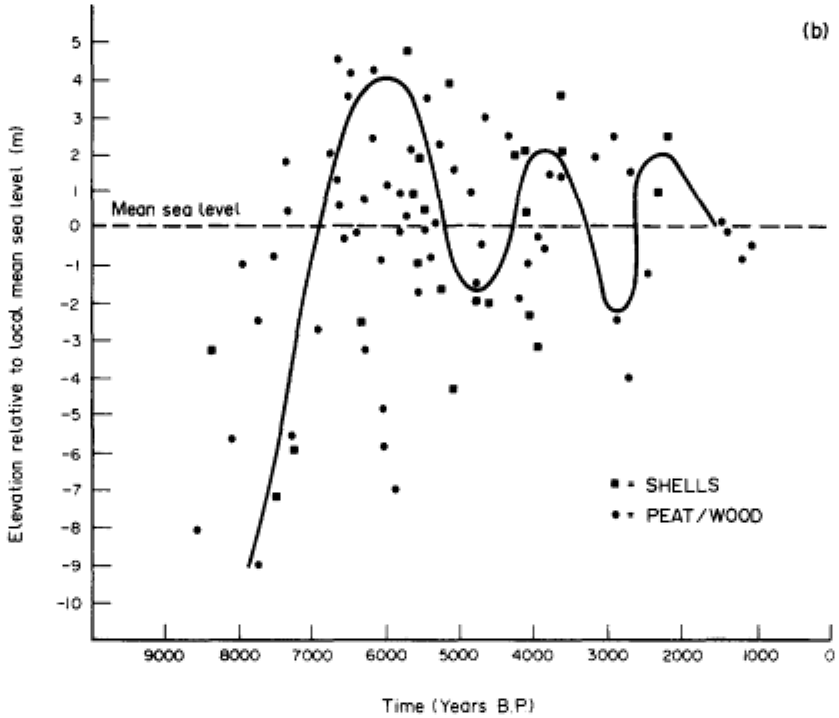

Figure 6 Holocene sea-level curve for Thailand using mean local sea level (Sinsakul 1992).

2.3 Study area

The study area is an open pit (13° 32.145'N to 13° 32.155'N and 100° 21.684'E to 100° 21.725'E) located 5 km west of the Phanthai Norasing subdistrict administrative organization office, Samut Sakhon Province, Thailand, and approximately 4.8 km north of the upper Gulf of Thailand (Figure 7). The open pit is approximately 25.48 m depth below the surface, covering approximately 0.42 km^2. Sediment samples were taken from 25.48 – 7.2 m depth below the surface. The profile above 7.2 m below the surface was not here including because of soil slump and possible disturbed by the pit construction. The environment surrounding the open pit was mostly occupied by community and shrimp farms (Figure 8). *Suaeda maritima* was a plant that was mostly found near the open pit.

Whereas *Rhizophora sp.* and *Nypa fruticans* were found in a tidal creek surrounding the study site.

Samut Sakhon Province is located in the lower central plain of Thailand, north of the upper Gulf of Thailand. The average elevation of this area is 2 m above the present mean sea level (Sinsakul, 2000). The lower central plain deposits were a complex sequence of alluvial, fluvial, and deltaic sediments of Mae Klong, Tha Chin, Chao Phraya, and Bank Pakong rivers (Tanabe et al., 2003). According to the general geological information, the lower central plain is overlaid on more than 2000 m thick of Tertiary and Quaternary sediments. The western and eastern plain margins are associated with alluvial fans and terraces (Sinsakul, 2000) (Figure 9). The geomorphology of the lower central plain system consists of delta plain, tidal flat (mud flat), river mouth flat, delta front, and delta (Tanabe et al., 2003).

The Asian monsoon plays a key role in the climate in Thailand (Chabangborn et al., 2020). The southwest monsoon brings humid air masses from the Indian Ocean and increased precipitation from mid-May to October. The northeast monsoon prevails, leading to cool and dry conditions between October and February. In February and early May, Thailand is under the influence of southerly and southeasterly winds, increasing temperature. The mean annual precipitation in Samut Sakhom is 1200-1400 mm (Thai Meteorological Department, 2022). The highest rainfall is in September, which is 200-300 mm. The mean annual temperature is 28-30 $^{\circ}$C (Thai Meteorological Department, 2022).

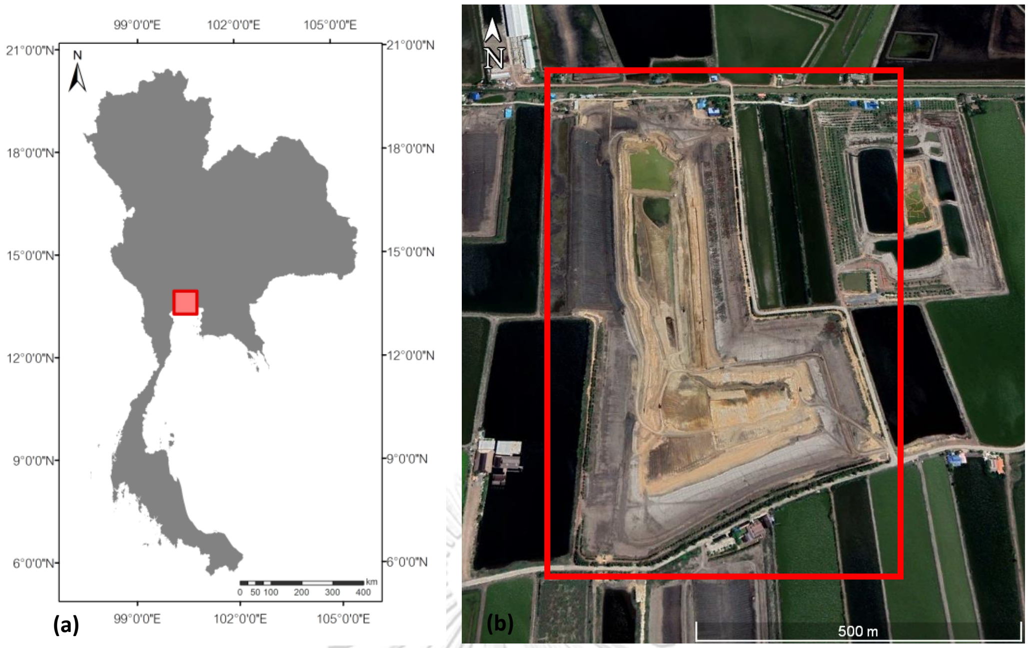

Figure 7 (a) Location map of the study site on Samut Sakhon province in the upper Gulf of Thailand, (b) study site is an open pit in Samut Sakhon province.

Figure 8 The open pit and the environment surrounding in Samut Sakhon (a) facing southwest, (b) facing south

(b)

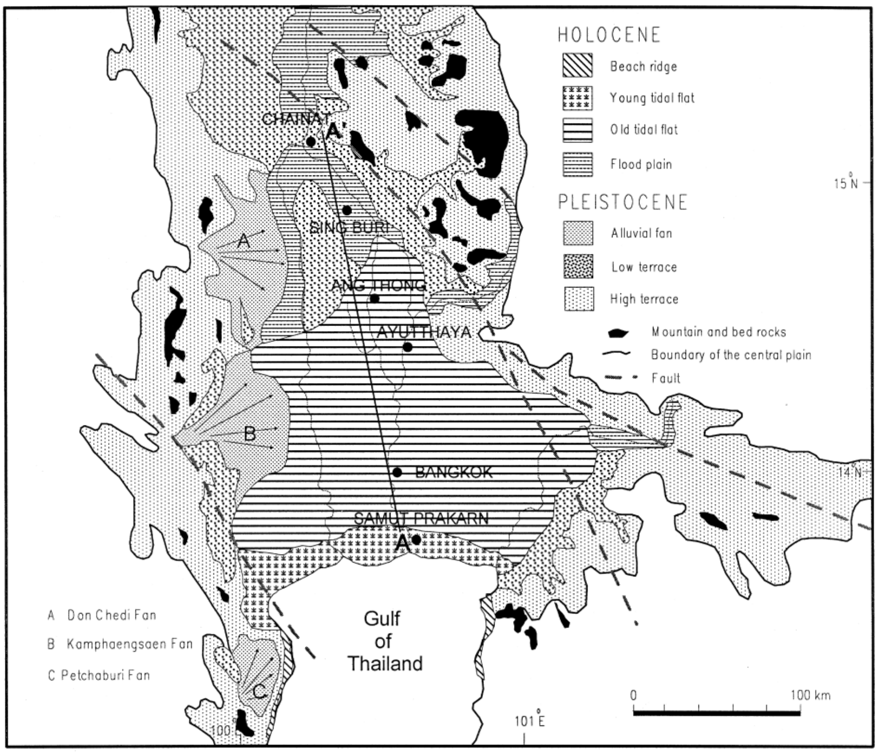

Figure 9 Geological map shows the Quaternary deposits in the Lower Central Plain, the Gulf of Thailand (Sinsakul, 2000).

CHAPTER 3
METHODOLOGY

3.1 Sample collection

Sediment samples were collected from an open pit in Samut Sakhon Province by hammering the 2 cm diameter and 5 cm long PVC tubes in the sediment layers (Figure 10). Sediment samples were taken every 10 centimeters from each soil layer at the bottom of the pond until the top of the site (Figure 11). Discontinuity of soil profile in the pond was insufficient therefore collecting samples must to taken from 4 zones including zones 1, 2, 3, and 4 around the pond to complete all soil profiles. Where zone 1 (Z1) includes sediment from 25.48-19.74 m DBS in unit A-D, zone 2 (Z2) includes sediment from 19.67-17.37 m DBS in the top of unit D to unit E, zone 3 (Z3) includes sediment from 14.93-14.29 in unit F-G, and zone 4 (Z4) includes sediment from 14.26-7.20 in unit H-I. The sediment samples were placed in PVC tubes, transported to the Department of Geology, Chulalongkorn University, and kept for further analysis. The laboratory work included a detailed lithostratigraphic description of the sediment sequences, X-ray fluorescence, pollen analysis, loss on ignition, and radiocarbon dating.

Level measurement was measured by using an Automatic level where the reference level was approximately the same level as Samut Sakhon Rural Road 2004. The open pit is around 18.28 m thick with the level of the bottom 25.48 and the top 7.20 m. The unit of m depth below the surface (m DBS) was used in this study where the surface means the Samut Sakhon Rural Road 2004 level.

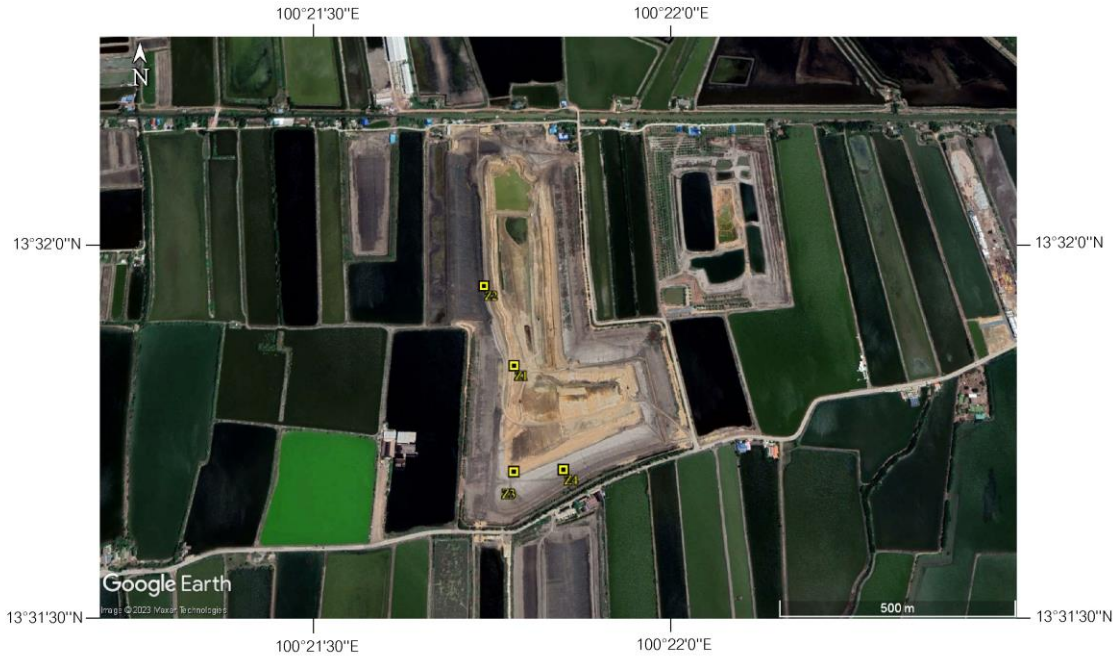

Figure 10 Satellite image from Google Earth showing 4 sampling size zones in the yellow dot in the open pit.

Figure 11 Sampling method using PVC tube hammering into sediment every 10 cm interval.

3.2 Laboratory works

One hundred forty-five samples were divided and analyzed in the laboratory including X-ray fluorescence, loss on ignition, grain size analysis, pollen analysis, and radiocarbon dating detailed in Table 3.

Table 3 Summary table of samples analyzed in the laboratory

Sample no.	m DBS	XRF	LOI	Grain size analysis	Pollen analysis
1	25.48	✓	✓	✓	✓
2	25.38	✓	✓		
3	25.28	✓	✓	✓	
4	24.98	✓	✓		✓
5	24.88	✓	✓	✓	
6	24.79	✓	✓		
7	24.70	✓	✓	✓	✓
8	24.41	✓	✓		✓
9	24.32	✓	✓	✓	✓
10	24.23	✓	✓		✓
11	24.13	✓	✓	✓	
12	24.04	✓	✓		
13	23.94	✓	✓	✓	✓
14	23.85	✓	✓		
15	23.76	✓	✓	✓	
16	23.66	✓	✓		✓
17	23.57	✓	✓	✓	✓
18	23.47	✓	✓		
19	23.38	✓	✓	✓	✓
20	23.19	✓	✓		✓
21	23.10	✓	✓	✓	
22	23.00	✓	✓		✓
23	22.91	✓	✓	✓	
24	22.82	✓	✓		✓
25	22.72	✓	✓	✓	✓
26	22.63	✓	✓		

27	22.53	✓	✓	✓	
28	22.44	✓	✓		✓
29	22.35	✓	✓	✓	✓
30	22.25	✓	✓		
31	22.16	✓	✓	✓	
32	22.06	✓	✓		
33	21.64	✓	✓	✓	
34	21.54	✓	✓		
35	21.44	✓	✓	✓	
36	21.34	✓	✓		✓
37	21.24	✓	✓	✓	
38	21.14	✓	✓		
39	21.04	✓	✓	✓	
40	20.94	✓	✓		
41	20.84	✓	✓	✓	
42	20.74	✓	✓		
43	20.64	✓	✓	✓	✓
44	20.54	✓	✓		
45	20.44	✓	✓	✓	
46	20.34	✓	✓		
47	20.24	✓	✓	✓	
48	20.14	✓	✓		
49	20.04	✓	✓	✓	
50	19.94	✓	✓		
51	19.84	✓	✓	✓	
52	19.74	✓	✓		✓
53	19.67	✓	✓	✓	
54	19.57	✓	✓		✓
55	19.47	✓	✓	✓	✓

56	19.37	✓	✓		✓
57	19.27	✓	✓	✓	
58	19.17	✓	✓		✓
59	19.07	✓	✓	✓	
60	18.97	✓	✓		✓
61	18.57	✓	✓	✓	✓
62	18.47	✓	✓		
63	18.37	✓	✓	✓	
64	18.27	✓	✓		
65	18.17	✓	✓	✓	
66	18.07	✓	✓		
67	17.97	✓	✓	✓	✓
68	17.87	✓	✓		
69	17.77	✓	✓	✓	
70	17.67	✓	✓		
71	17.57	✓	✓	✓	
72	17.47	✓	✓		
73	17.37	✓	✓	✓	✓
74	14.93	✓	✓		✓
75	14.90	✓	✓	✓	
76	14.87	✓	✓		✓
77	14.84	✓	✓	✓	
78	14.81	✓	✓		✓
79	14.74	✓	✓	✓	✓
80	14.71	✓	✓		
81	14.68	✓	✓	✓	
82	14.64	✓	✓		
83	14.61	✓	✓	✓	
84	14.58	✓	✓		

85	14.55	✓	✓	✓	
86	14.52	✓	✓		✓
87	14.48	✓	✓	✓	
88	14.45	✓	✓		
89	14.42	✓	✓	✓	
90	14.39	✓	✓		
91	14.35	✓	✓	✓	
92	14.32	✓	✓		
93	14.29	✓	✓	✓	✓
94	14.23	✓	✓		✓
95	14.09	✓	✓	✓	
96	13.96	✓	✓		✓
97	13.83	✓	✓	✓	
98	13.70	✓	✓		✓
99	13.56	✓	✓	✓	✓
100	13.43	✓	✓		
101	13.30	✓	✓	✓	✓
102	13.17	✓	✓		
103	13.03	✓	✓	✓	✓
104	12.90	✓	✓		
105	12.77	✓	✓	✓	✓
106	12.64	✓	✓		
107	12.50	✓	✓	✓	✓
108	12.37	✓	✓		
109	12.24	✓	✓	✓	✓
110	12.11	✓	✓		
111	11.97	✓	✓	✓	✓
112	11.84	✓	✓		
113	11.71	✓	✓	✓	✓

114	11.58	✓	✓		
115	11.44	✓	✓	✓	✓
116	11.31	✓	✓		
117	11.18	✓	✓	✓	✓
118	11.05	✓	✓		
119	10.91	✓	✓	✓	✓
120	10.78	✓	✓		
121	10.65	✓	✓	✓	✓
122	10.52	✓	✓		
123	10.38	✓	✓	✓	✓
124	10.25	✓	✓		
125	10.12	✓	✓	✓	✓
126	9.72	✓	✓		✓
127	9.59	✓	✓	✓	
128	9.46	✓	✓		✓
129	9.32	✓	✓	✓	
130	9.19	✓	✓		✓
131	9.06	✓	✓	✓	
132	8.93	✓	✓		✓
133	8.79	✓	✓	✓	
134	8.66	✓	✓		✓
135	8.53	✓	✓	✓	
136	8.40	✓	✓		✓
137	8.26	✓	✓	✓	
138	8.13	✓	✓		✓
139	8.00	✓	✓	✓	
140	7.87	✓	✓		✓
141	7.73	✓	✓	✓	
142	7.60	✓	✓		✓

143	7.47	✓	✓	✓	
144	7.34	✓	✓		✓
145	7.20	✓	✓	✓	

3.2.1 X-Ray fluorescence

The consecutive 10 cm sediment samples were dried at 105°c for 12 hours for XRF analysis. The dried samples were ground in order to be homogeneous. Subsequently, sediment samples were put into a plastic crucible (Figure 12), and measured chemical compositions by using the handheld X-ray Fluorescence (XRF) model Olympus Vanta XRF series to assess the relative variabilities of each element (Figure 13). The concentrations of 39 elements (i.e., P, S, Cl, K, Ca, Ti, V, Cr, Mn, Fe, Co, Ni, Cu, Zn, As, Se, Rb, Sr, Y, Zr, Nb, Mo, Ag, Cd, Sn, Sb, Ba, La, Ce, Pr, Nd, Ta, W, Au, Hg, Pb, Bi, Th, and U) were detected by the handheld XRF. However, the concentrations of P, Cr, Co, Se, Mo, Ag, Cd, Sn, Sb, La, Ce, Pr, Nd, Ta, W, Au, Hg, Bi, Th, and U did not reach the instrumental detection limit and excluded for the further analysis.

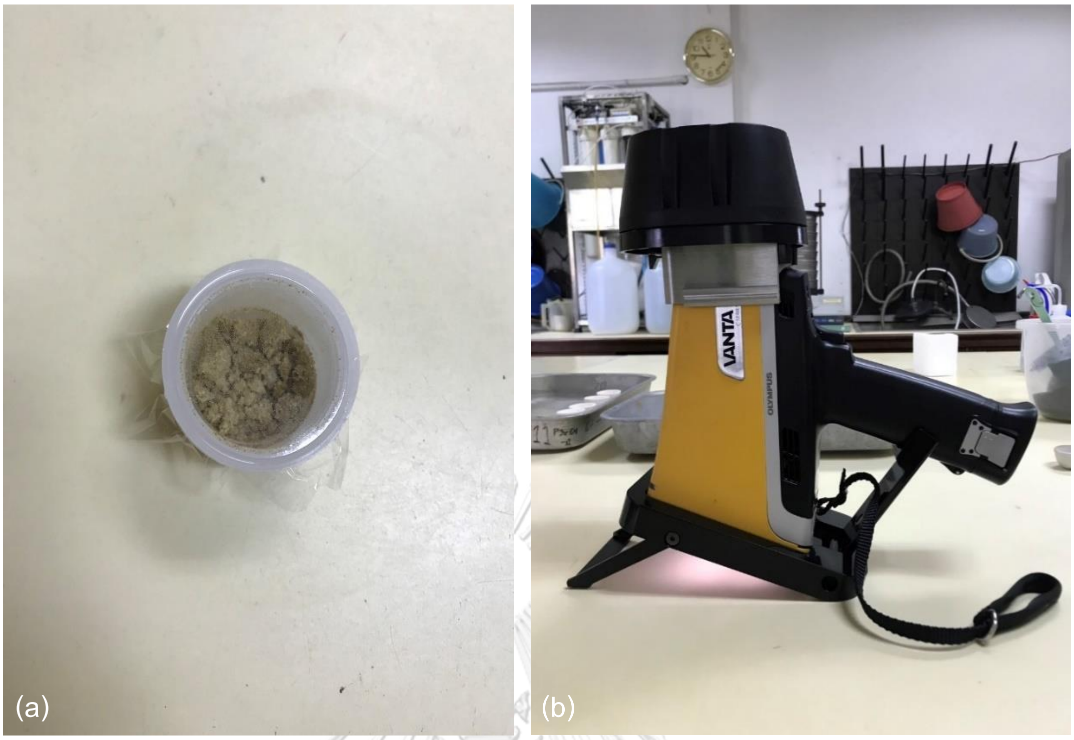

Figure 12 (a) Sediment sample in plastic crucible for XRF measurement, (b) handheld X-ray fluorescence analyzer model Olympus Vanta XRF series.

3.2.2 Loss on ignition (LOI)

The consecutive 10 cm samples were prepared for the LOI followed the procedure of Heiri et al., (2001). Crucibles and approximately 3 cm^3 of sediment samples were weighed and then dried at 105ºC for 12 hours. Subsequently, the dried samples were combusted at 550ºC for 6 hours (Figure 14).

Calculation of the relative organic carbon content can be estimated by the percentage of weight loss at 550ºC following the equation (1).

$$LOI_{550} = \frac{DW_{105} - DW_{550}}{DW_{105}} \times 100$$

(1)

Where LOI_t = weight loss on ignition at t ºC (g)

DW_t = dry weight of samples at t ºC (g)

Then, the samples were combusted at 950ºC for 3 hours in order to eliminate carbonate content in the form of CO_2. The weight loss at 950ºC can be calculated following equation (2).

$$LOI_{950} = \frac{DW_{550} - DW_{950}}{DW_{105}} \times 100 \tag{2}$$

Combustion at 950ºC (3), in order to transfer $CaCO_3$ in the sample into CO_2 and CaO. CO_2 is the weight loss. Consequently, the weight loss at 950ºC was multiplied by 2.27 in order to assess the carbonate content ($CaCO_3$) (3).

$$CaCO_3 \rightarrow CaO + CO_2$$

$$\frac{CaCO_3}{CO_2} = \frac{MW_{CaCO_3}}{MW_{CO_2}} = \frac{100.086\ g/mol}{44.009\ g/mol} = 2.27 \tag{3}$$

Where MW = Molecular weight (g/mol)

Figure 13 Crucible in a furnace for Loss on ignition analysis.

3.2.3 Grain Size Analysis

Seventy-three samples for the grain size analysis were prepared for each consecutive 10 cm depth following Rowell (2014).

3.2.3.1 Pretreated samples

Each subsample was treated by 20 ml of 10% (v/v) HCl, 20 ml of 10 %, and 30% H_2O_2 in order to eliminate carbonate and organic contents, respectively (Figure 14). The prepared samples were cleaned by deionized water 3 times and dried in an oven for 12 hours. Dried sediment samples were ground to break up the sediment into a smaller size.

The samples were eventually analyzed for the grain size distribution by laser diffraction technique by Horiba model Partica LA-960V2 Laser Scattering Particle Size Distribution Analyzer at the Department of Marine, Faculty of Science, Chulalongkorn University (Figure 14).

The grain size distribution was calculated to mean size particle by the following equation (5).

$$D[4,3] = \frac{\sum_i^n D_i^4 v_i}{\sum_i^n D_i^3 v_i} \tag{5}$$

Where D [4,3] = the mean diameter over volume

D_i = mean of dacile i

v_i = dacile i

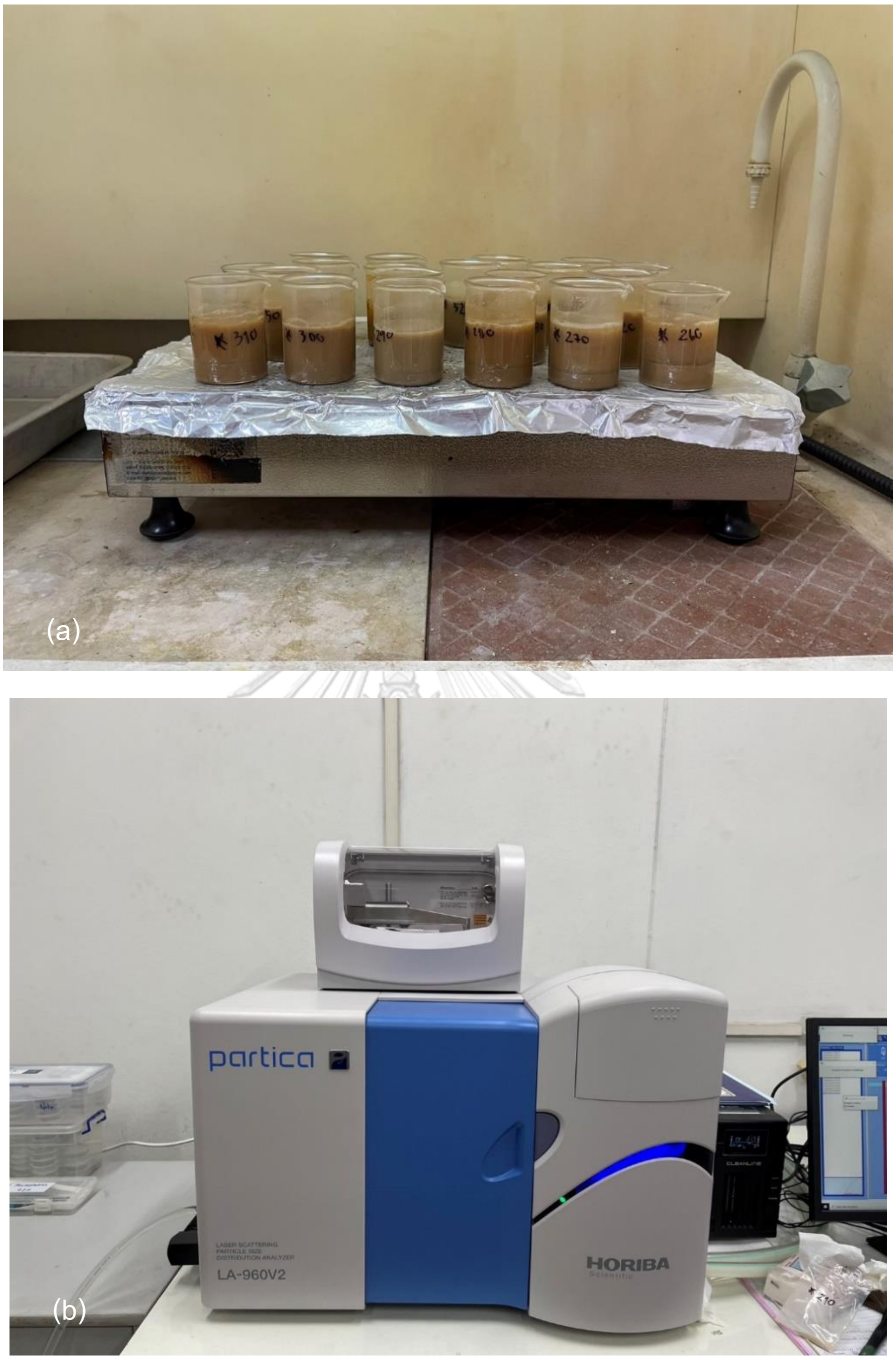

Figure 14 (a) The process of pretreating sediment sample with H_2O_2 to eliminate organic content, (b) Horiba model Partica LA-960V2 Laser Scattering Particle Size Distribution Analyzer.

3.2.4 Pollen analysis

Sixty sediment samples were prepared based on Ellison (2008). Subsamples from the bottom, middle, and top of each sediment layer were selected for pollen analysis.

3.2.4.1 Samples digestion

Subsamples were taken about 1 cm^3, treated by 10 ml of 10% KOH, and heated on a hotplate to disperse the sediment (Figure 15). Subsamples were subsequently sieved with a mesh size of 0.2 mm (Figure 15). The sieve remains were washed by deionized water multiple times

For the Acetolysis method, subsamples were treated by glacial acetic (CH_3COOH), and mixed acetic anhydride (CH_3CO_2O) and 96% sulfuric acid (H_2SO_4).

3.2.4.2 Heavy Liquid

Heavy liquid, Sodium polytungstate ($3Na_2WO_4 \cdot 9WO_3 \cdot H_2O$) which density is 2.0 g/cm^3, was added into subsamples, and water was added, respectively. The prepared samples were centrifuged at the speed of 2000 rpm for 2 minutes. Consequently, the heavy liquid with pollen was separated from the solvent by using a dropper. The samples were washed by 95% alcohol, added silicone oil then dried at 60 ºC for 12 hours to eliminate alcohol.

Eventually, the samples were mouth on glass slides using Paraffin and pollens were identified under stereomicroscope based on their morphology including aperture, sculpture, and size (Figure 15). Pollens were identified in regard to Punwong (2007).

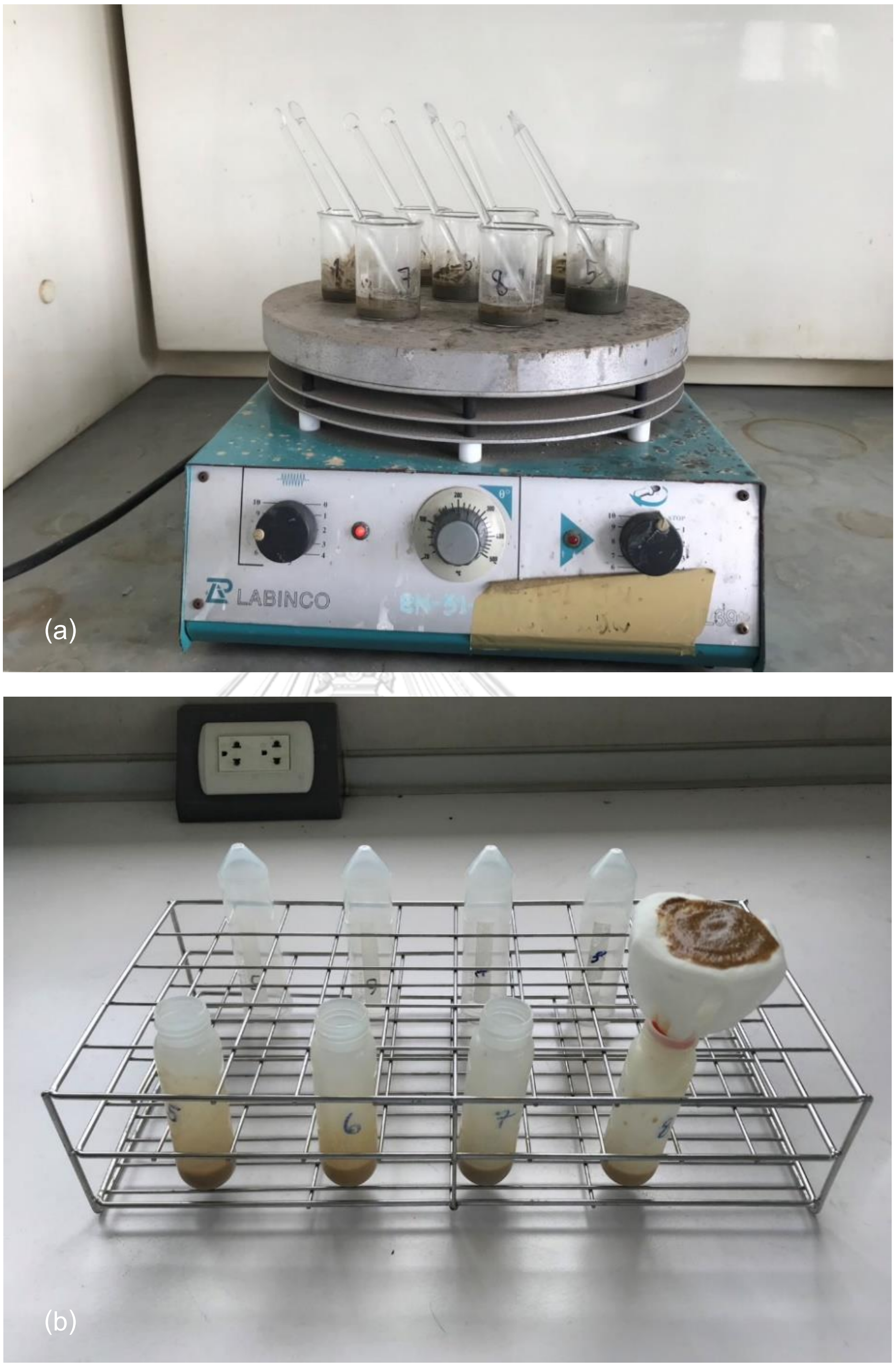
(a)
LABINCO
(b)

Figure 15 The process of preparing the sample for pollen sample analysis, (a) sediment samples digestion by KOH and heat with a hot plate, (b) sample sieving sample through 0.2 mm mesh, (c) pollen samples mouthed on glass slides using Paraffin.

3.2.5 Radiocarbon dating

Radiocarbon dating in this study has focused on bulk sediment and shells. Bulk sediment samples were dried at 110°c for 12 hours and then let it cool down. Dried bulk sediment was ground into a smaller size, pack into aluminum foil. Shell samples were picked up by forceps and cleaned with deionized water multiple times. Shell samples were dried at 60°c for 12 hours (Figure 16). The dating samples were packed into aluminum foil and then prepared samples were sent to analyze by using the Accelerated Mass Spectrometer (AMS) at direct AMS, the USA (Figure 16).

The radiocarbon dating results from bulk sediment were calibrated by using a calibration curve of InCal20 (Plicht et al., 2020) while shells were calibrated by MARINE20 with -174 Marine error and 70 uncertainty (Southorn et al., 2002). The age-depth model was constructed for CP-4 by interpolation between the adjacent dating results.

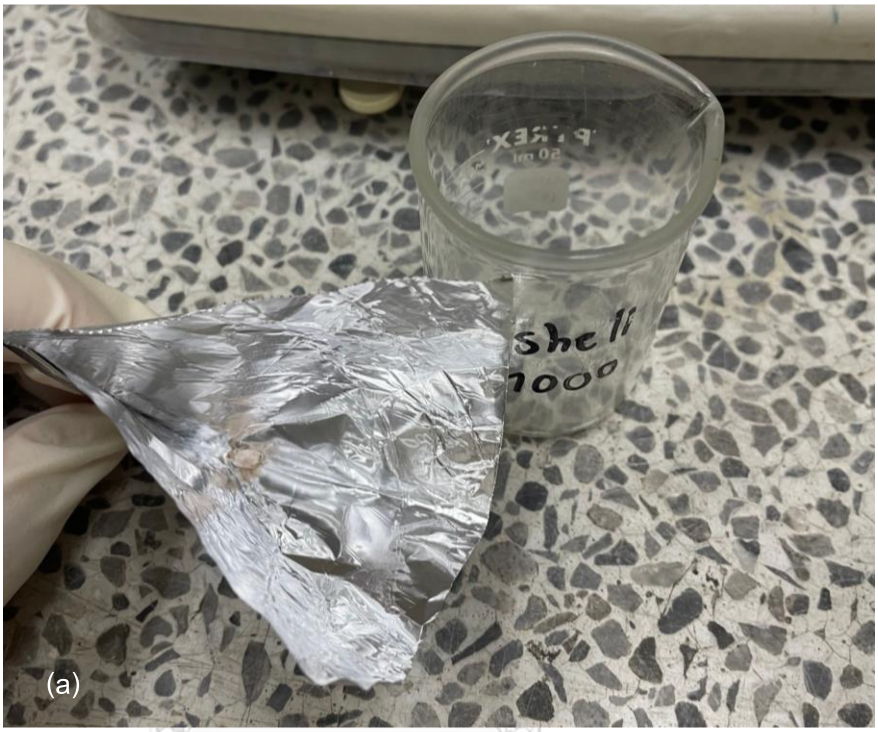

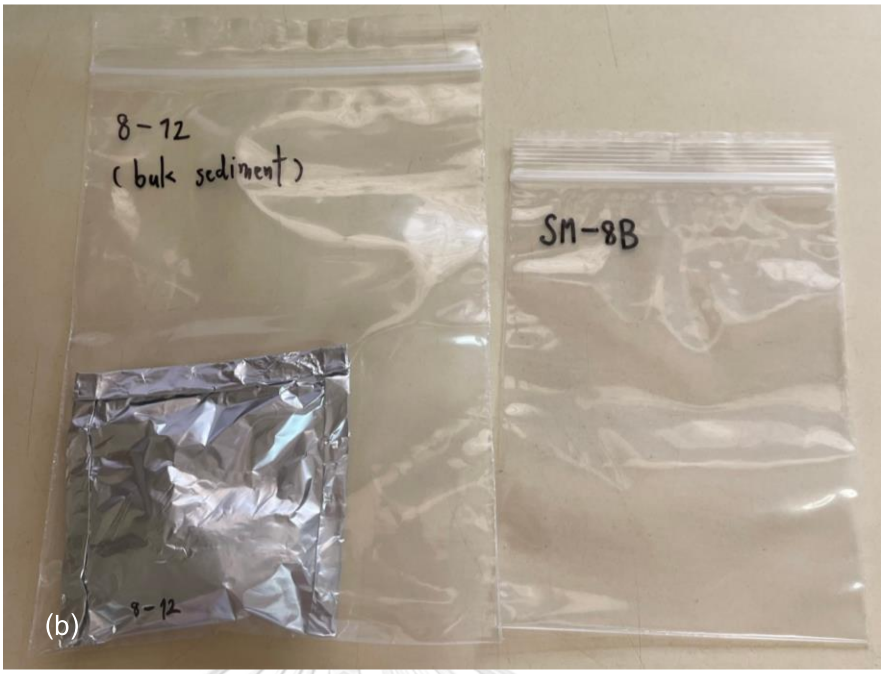

Figure 16 (a) Shell sample for radiocarbon dating after being cleaned by deionized water and dry, (b) bulk sediment sample in foil package prepared for sent to dating.

CHAPTER 4
RESULTS

4.1 Stratigraphic Description of Samut Sakhon Site

The sedimentary sequence from the open pit is approximately 18.3 m thick, extending from 25.48 to 7.20 m DBS. According to the sedimentary description during the field survey, this sequence can be divided into 9 units, i.e., units A to I from the bottom to top, consisting of 14 layers (Table 4).

Unit A

Unit A is well-compacted light grey clay with a paucity of organic matter. This unit is laid down at the lowermost part of the sedimentary sequences. It extends below approximately 24.70 m DBS. The obvious high silt fraction can be observed in the upper part of this unit before gradual transfers to unit B (Table 4 and Figure 17).

Figure 17 The well compaction light grey clay of unit A.

Unit B

Unit B is a relatively thin layer of brown clayey silt intervened between the light grey clay of unit A and the oxidized grey clayey silt of unit C. It is approximately 0.38 m thick and extends between 24.70 and 24.32 m DBS (Table 4 and Figure 28).

Figure 18 The brown silty clay of Unit B.

Unit C

Unit C consists of oxidized grey clayey silt (layer 3) and grey clayey silt with more clay content layer (layer 4). The purple color of these sediments is possibly caused by oxidation. This unit is approximately 1 m thick and can be found at 24.32-23.38 m DBS (Table 4 and Figure 19).

Figure 19 The grey clayey silt with purple oxidized surface of unit C.

Unit D

Unit C is overlaid by unit D, which is interbedded between the brown clayey silt layers (Table 4 and Figure 20). Unit D can be divided into 5 layers, i.e., layers 5-9 from the bottom to top. This unit is approximately 4.4 m thick and extends from 23.38-19.00 m DBS. It is punctuated by a layer of clayey silt with gravel (approximately 10-15%) at 19.70-19.50 m DBS. Regarding the XRD analysis at the Department of Geology, Chulalongkorn University, the gravel is entirely composed of Sio_2, and $CaCO_3$, indicating the caliche layer

(Alptekin & Hatipoglu, 2018) (Figure 21). The limestone mountain is not available in the study area and vicinity area. In addition, $CaCO_3$ is a low concentration in the sediments from Tha Chin and Chao Phraya Rivers (Hassain et al., 2017). Since shells and shell fragments are abundant in the upper part of the sediment sequence, the precipitated $CaCO_3$ gravel is possibly caused by infiltration of hardwater dissolved from the upper shell layer.

Figure 20 The interbedded between the brown clayey silt of unit D.

Figure 21 Sediment in unit D and a presence Caliche layer.

Unit E

Sediment in Unit E is laminated light grey clay, which is approximately 19.00–17.37 m DBS. The sediments in this layer are characterized by hard and well compaction, making it difficult to mound by PVC pipe (Table 4 and Figure 22).

The upper part of unit E is a road for transportation in the open pit close to the slump sediments. To avoid contamination by younger sediments, the sampling site was moved to approximately 500 m to the west, making the loss of information approximately 2.5 m thick.

Figure 22 The laminated light grey clay of unit E.

Unit F

The sediments in unit F are purple clay, which is possibly oxidized. This unit can be found at approximately 14.70 m DBS (Table 4 and Figure 23).

Unit G

The purple clay in unit F gradually transfers to the greenish-dark grey clay of unit G. It is approximately 0.22 m thick at 14.70–13.33 m DBS. In unit G, shells and shell fragments can be found in the sediments (Figure 23). The shells and shell fragments increase by 5-10% from the bottom to the top of this unit (Table 4).

Unit H

Unit G is gradually changed to the dark grey clay of unit H. The shells and shell fragments are approximately 5% in this unit (Figure 24 and 25). Unit H is 0.67 m thick, approximately 13.33–12.66 m DBS (Table 4).

Figure 23 The boundary between the greenish-dark grey clay of unit G and the dark grey clay of unit H.

Unit I

Unit I is the uppermost unit of the sedimentary sequences. This unit is relatively thicker than the other units, which is at least 5.46 m thick. It is composed of dark brown clayey silt. Shells and shell fragments are abundant in the middle of unit I, approximately more than 15%. Unit I extends from 12.66 to 7.20 m DBS (Table 4 and Figure 24, 25). Summary of the sedimentary sequence in Samut Sakhon show in Figure. 26.

Figure 24 The dark brown clayey silt in unit I.

Figure 25 The shell layer presence in units G to I.

Table 4 Lithostratigraphic description of sediment sequence of the open pit at Samut Sakhorn consist of 9 unit and 14 layers.

m DBS	Lithostratigraphy description	Unit	Layer
7.20 - 12.66	Dark brown clayey silt	I	14
12.66 - 13.33	Dark grey clay	H	13
13.33 - 14.67	Greenish-dark grey clay	G	12
14.67 - 14.89	Purple clay (oxidized)	F	11
	hiatus		
17.37 - 18.97	Laminate light grey clay	E	10
18.97 - 19.47	Brown clayey silt		9
19.47 - 19.74	Brown clayey silt with gravel and Caliche layer		8
19.74 - 22.44	Brown clayey silt (more clay)	D	7
22.44 - 22.82	Brown clayey silt		6
22.82 - 23.38	Brown clayey silt (oxidized)		5
23.38 - 23.66	Grey clayey silt (more clay and oxidized)	C	4
23.66 - 24.32	Grey clayey silt (oxidized)		3
24.32 - 24.70	Brown clayey silt	B	2
24.70 - 25.48	Light grey clay	A	1

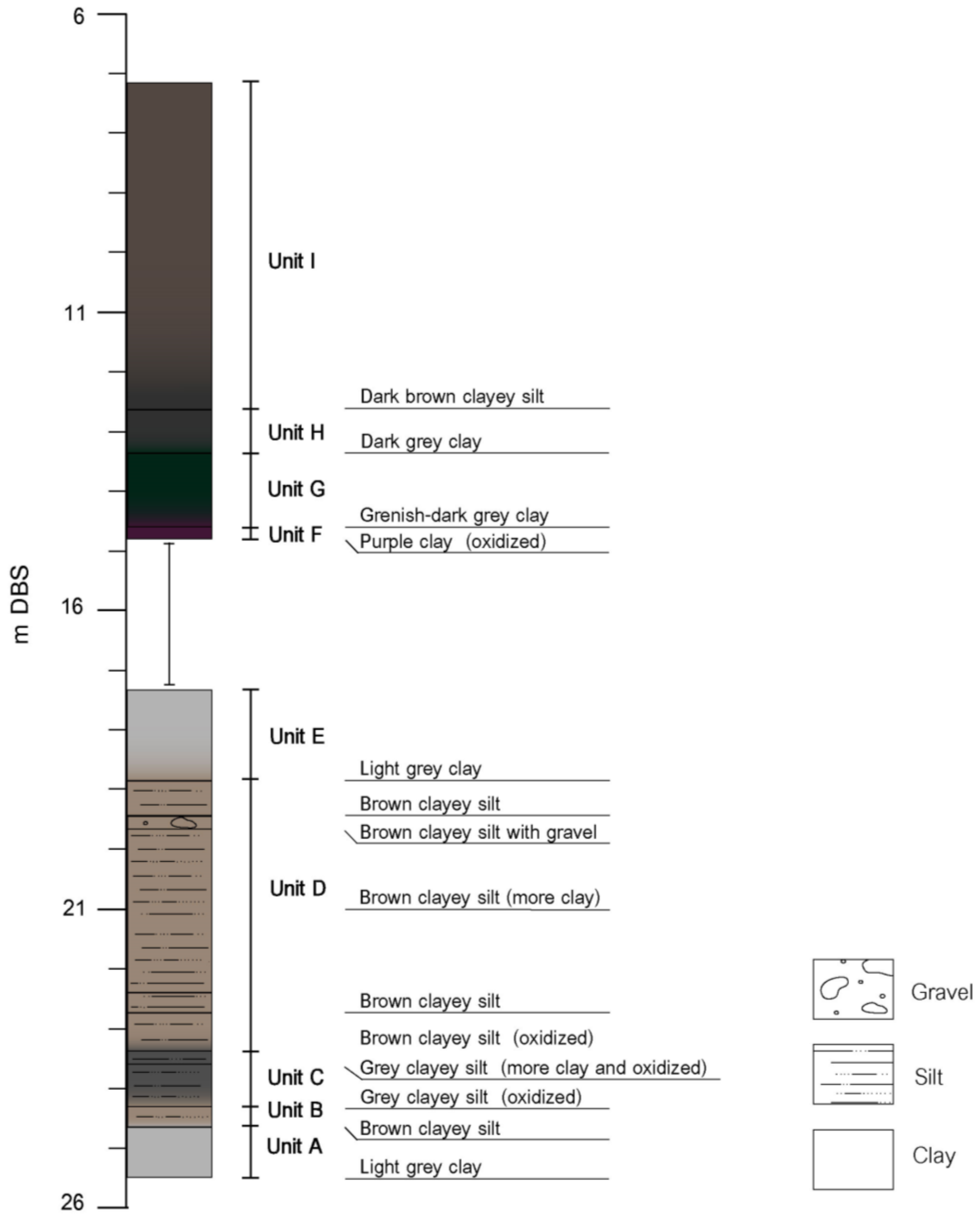

Figure 26 Lithostratigraphic column of sediment sequence of the open pit at Samut Sakhon.

4.2 Loss on ignition (LOI)

The consecutive 10 cm depth of sediment samples were combusted at 550°C (LOI550) and 950°C (LOI950) to achieve the qualitative changes in organic and carbonate content.

The LOI550 is approximately 7.5% in units A and B (Figure 27). It abruptly decreases to 5% at the boundary between units B and C before gradually increasing to 7.5% at 22.00 m DBS (the lower part of unit D) (Figure 27). The LOI550 suddenly declines and reaches 2.5% at 22.00-21.00 m DBS (Figure 27). It is a slight change of 2.5% from 21.00 m DBS to the upper part of unit D (Figure 27). The LOI550 abruptly increases to 10% in unit E. In units F to I, the LOI550 generally increases from 10 to 20% (Figure 27).

The LOI950 varies from 2.5% to 5% (Figure 27). The variation of the LOI950 is approximately analogous to that of the LOI550, except for units B to D (Figure 27). The LOI950 gradually decreases from 2.5% to 1% in units B to D (Figure 27). In addition, the LOI950 significantly increases and reaches its maximum of 12.5% in the caliche layer (Figure 27).

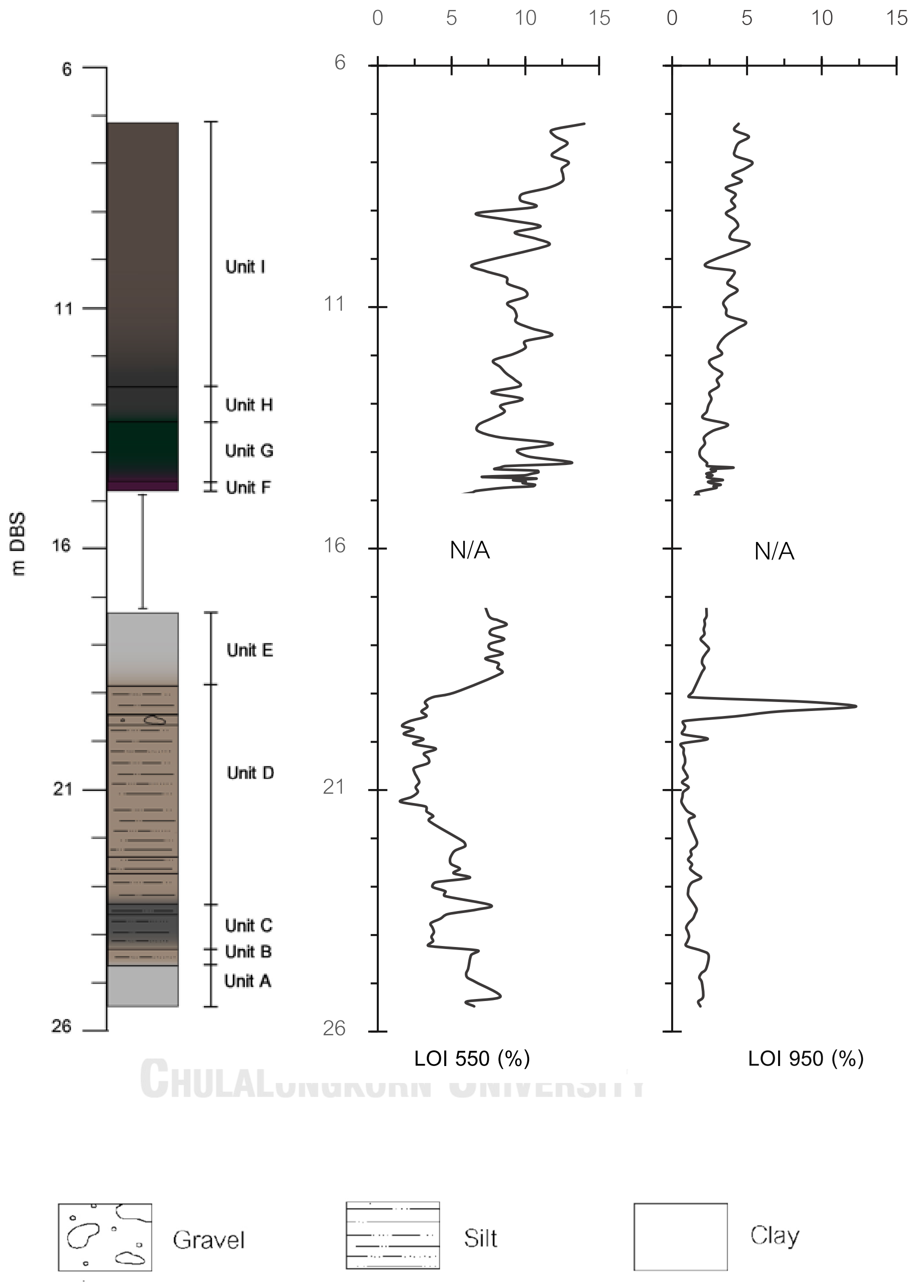

Figure 27 Comparison of lithostratigraphy (left), and profile of LOI550 (middle) and LOI950 (right) of sediment sequence of the open pit at Samut Sakhon.

4.3 Grain size analysis

The sediment sequence of the open pit at Samut Sakhon is generally composed of a silt fraction of 75%, 20% sand, and 5% clay (Figure 28).

In units A to the lower part of unit D (24.70-22.16 m DBS), the silt fraction is approximately 75% and the most predominant constitution. Sand component is 5% in units A and B, suddenly increases and reaches 40% in unit C, and varies from 20% to 40% in the lower part of unit D (24.13-22.16 m DBS) (Figure 28). In contrast, the clay fraction is 25% in units A and B, abruptly declines to less than 5% in the boundary between units B and C, and slightly increases to 15% in units B and the lower part of unit D (25.28-22.16 m DBS) (Figure 28).

The sand fraction suddenly increases and reaches 80%, while silt and clay components decrease by 75-20% and 20-5%, respectively, from 22.10 to 20.84 m DBS (Figure 28). The sedimentary components are a slight change of 80% sand, 20% silt, and less than 5% clay from 20.74 to 18.97 m DBS. The decrease in sand fraction consists of an increase in silt and clay components at 18.57-17.37 m DBS, before slight changes of 5% sand, 70% silt, and 25% clay in unit E (Figure 28).

Sand fraction increases from 10% to 20% in unit F, reaches 40% in unit G, decreases to 5% in units G and H, and gradually enhances by 5 to 40% in unit I. In units F to I, the silt component is generally 80%, except for 8.50 m DBS, which declines to 60%. The clay constituent is generally less than 5%, except for 14.00 and 11.50 m DBS, where it abruptly increases to 25% (Figure 28).

The volumetric mean diameter (D[4,3]) is less than 5 μm in units A and B. It slightly increases to 50 μm in unit C before declining to 10 μm in the lower part of unit D (23.50-22.16 m DBS) (Figure 28). In unit D, the volumetric mean diameter significantly increases and reaches its maximum of 200 μm at 20.74-18.97 m DBS (Figure 28). The volumetric mean diameter suddenly declines to resemble those in units A and B. In units F to I, the volumetric mean diameter gradually increases from 20 to 40 μm (Figure 28).

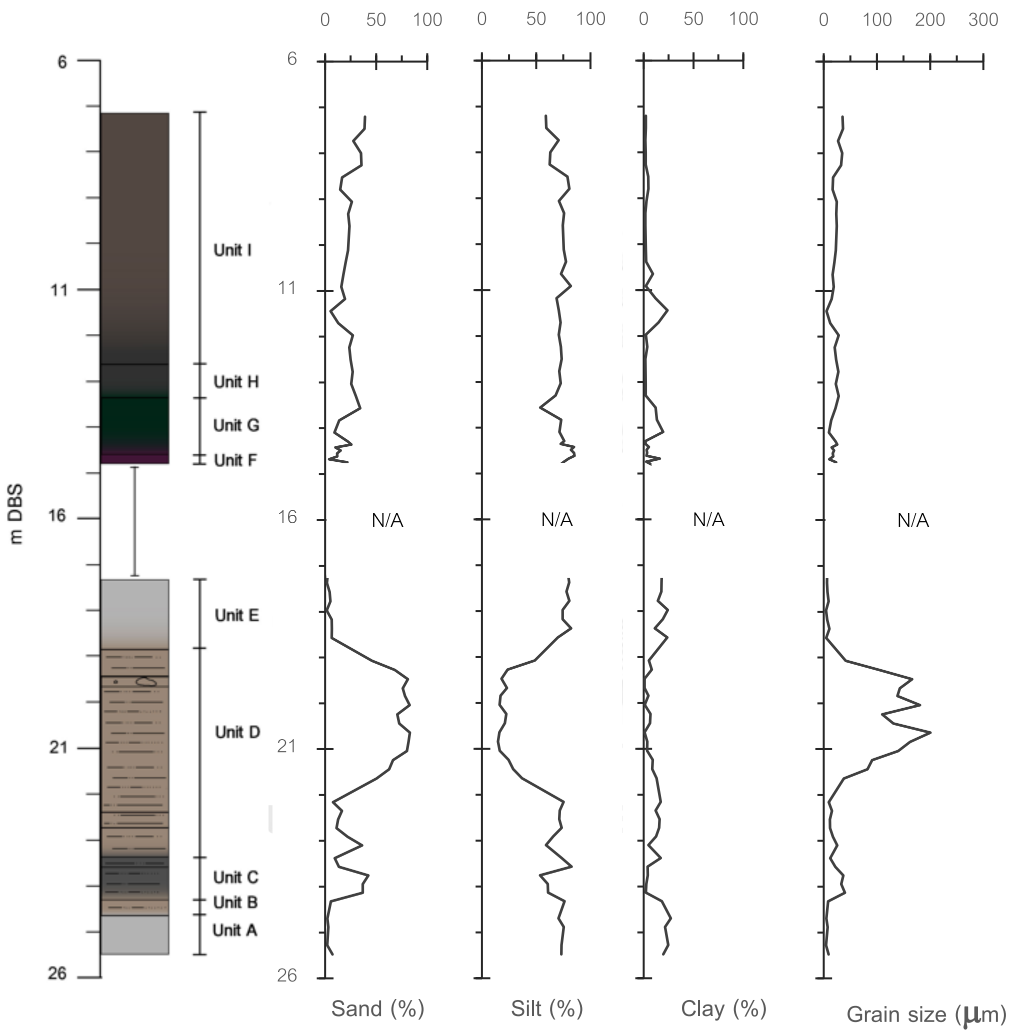

Figure 28 The lithostratigraphic column and percentage of sand, silt, and clay components, and volume metric mean grain size of the sediment sequence of the open pit at Samut Sakhon.

4.4 X-ray Fluorescence (XRF)

According to the XRF analysis, 39 elements of P, S, Cl, K, Ca, Ti, V, Cr, Mn, Fe, Co, Ni, Cu, Zn, As, Se, Rb, Sr, Y, Zr, Nb, Mo, Ag, Cd, Sn, Sb, Ba, La, Ce, Pr, Nd, Ta, W, Au, Hg, Pb, Bi, Th, and U can be detected by the handheld XRF. However, the continuous detectable elements consisting of Fe, Cl, K, Ca, S, Ti, Mn, Ba, Zr, Sr, Rb, and Zn are included in the further analysis (Figure 29).

The Fe, K, Ti, Zr, Rb, and Zn concentrations demonstrate the analogous pattern of variation. There are high concentrations of 26000, 13000, 3800, 400, 130, and 50 ppm (Figure 29) of Fe, K, Ti, Zr, Rb, and Zn, respectively, in units A to the lower part of unit D (23.50-22.16 m DBS). Fe, K, Ti, Zr, Rb, and Zn decreased to approximately 21000, 9000, 1200, 130, 90, and 20 ppm, respectively, at 20.74-18.97 m DBS (Figure 29). In unit E, they increase and approximately resemble those of unit A to the lower part of unit D. Fe, K, Ti, Zr, Rb, and Zn concentrations are insignificant changes of 27000, 10000, 2900, 350, 100, and 40 ppm, respectively, in units F to I (Figure 29).

Cl, Ca, and S concentrations in units A to E are 8000, 1200, and 200 ppm, respectively (Figure 29). They are significantly lower than those in units F to I, which are approximately 8000- 80000 ppm of Cl, 2900-30000 ppm of Ca, and 2200-30000 ppm of S (Figure 29). The exception is in the caliche layer, in which the Ca concentration significantly increases and reaches 140000 ppm (Figure 29).

Ba concentration is insignificant changes and varies from 200 ppm to 600 ppm. Mn concentration is relatively low, except at 20.74-18.97 m DBS, where it varies from 40 ppm to 18000 ppm (Figure 29). Sr concentration significantly changes from 90-200 ppm at 20.74-18.97 m DBS, and relatively increased 40-250 ppm from unit F-I (Figure 29).

The Principle Component Analysis (PCA) was used to assess the relationship between each element. The Kauser Meyer Olkin test (KMO) was 0.623, indicating an adequacy of PCA analysis. The eigenvalues were 4.5 and 2.3 on components 1 and 2, respectively, and the cumulative variance was 57.5% (Table 5). Therefore, the components 1 and 2 are selected in this study. The first principal component was ~37.9% of the total variance (Figure 30). It consists of K, Ti, Fe, Rb, and Zn (Table 6). The second principal component is ~19.6% of the total variance, consisting of S, Cl, Sr and Ca, opposing to Ba (Table 6 and Figure 30).

The elemental ratios are often applied for paleoclimatic and paleoceanographic reconstructions (e.g., Clift et al., 2014; Kylander et al., 2011). Among these ratios, Ti/Ca and Zr/Rb were proxies to assess terrigenous input and its intensity (Kylander et al., 2011; Hou et al., 2020; Mesa-Fernández et al., 2022). Titanium is normally delivered by terrigenous input, i.e., fluvial and eolian transportation (Hou et al., 2020), while calcium is originated by marine biogenic carbonate (Mesa-Fernández et al., 2022). Rubidium is common in mica and clay minerals (Kylander et al., 2011). Their strong absorption to clay minerals of Rubidium makes it immobile in the environment. Zirconium is generally found as zircon and enriched in silt (Kylander et al., 2011)

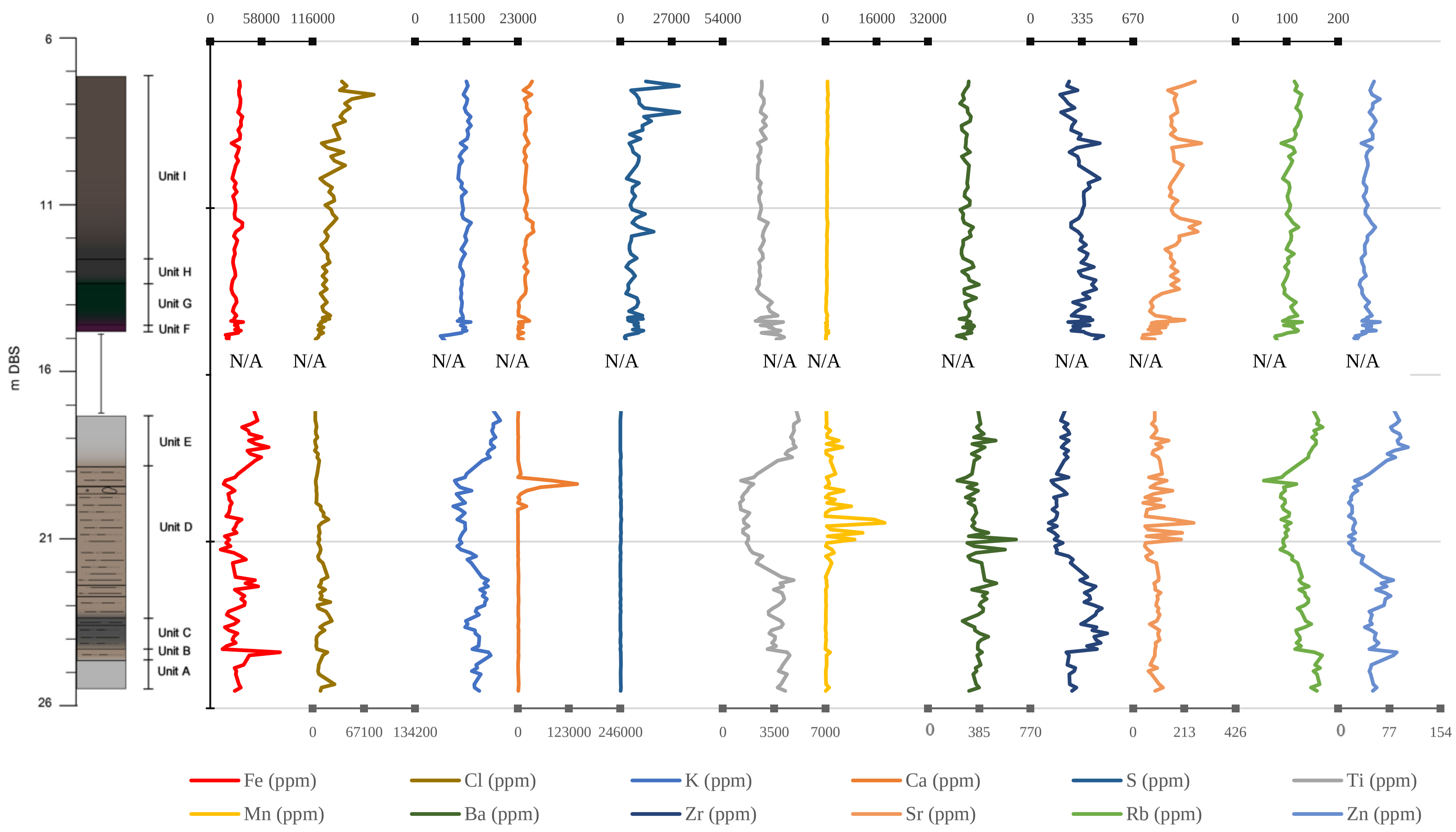

Figure 29 The lithostratigraphic column and concentration of selected elements of the sediment sequence of the open pit at Samut Sakhon.

Table 5 Total Variance Explained from PCA Analysis.

Total Variance Explained

	Initial Eigenvalues			Extraction Sums of Squared Loadings			Rotation Sums of Squared Loadings		
Component	Total	% of Variance	Cumulative %	Total	% of Variance	Cumulative %	Total	% of Variance	Cumulative %
1	4.55	37.93	37.93	4.55	37.93	37.93	4.16	34.70	34.70
2	2.35	19.61	57.54	2.35	19.61	57.54	2.70	22.50	57.20
3	1.71	14.25	71.80	1.71	14.25	71.80	1.75	14.59	71.80
4	.89	7.43	79.23						
5	.77	6.45	85.68						
6	.56	4.67	90.34						
7	.38	3.20	93.55						
8	.30	2.54	96.08						

9	.24	2.02	98.10
10	.11	.93	99.03
11	.09	.73	99.76
12	.03	.24	100.00

Extraction Method: Principal Component Analysis.

Table 6 Rotated Component Matrix from PCA analysis.

Rotated Component Matrix[a]			
	Component		
	1	2	3
S	-.06	.81	-.19
Cl	.04	.82	-.04
K	.90	-.25	.10
Ca	-.27	.58	.05
Ti	.81	-.23	-.39
Mn	-.10	-.01	.86
Fe	.85	.07	.17
Rb	.90	-.13	-.03
Sr	-.01	.79	.23
Zr	-.02	-.01	-.75
Ba	.38	-.50	.41
Zn	.96	.001	-.11

Extraction Method: Principal Component Analysis.

Rotation Method: Varimax with Kaiser Normalization.

[a] a. Rotation converged in 4 iterations.

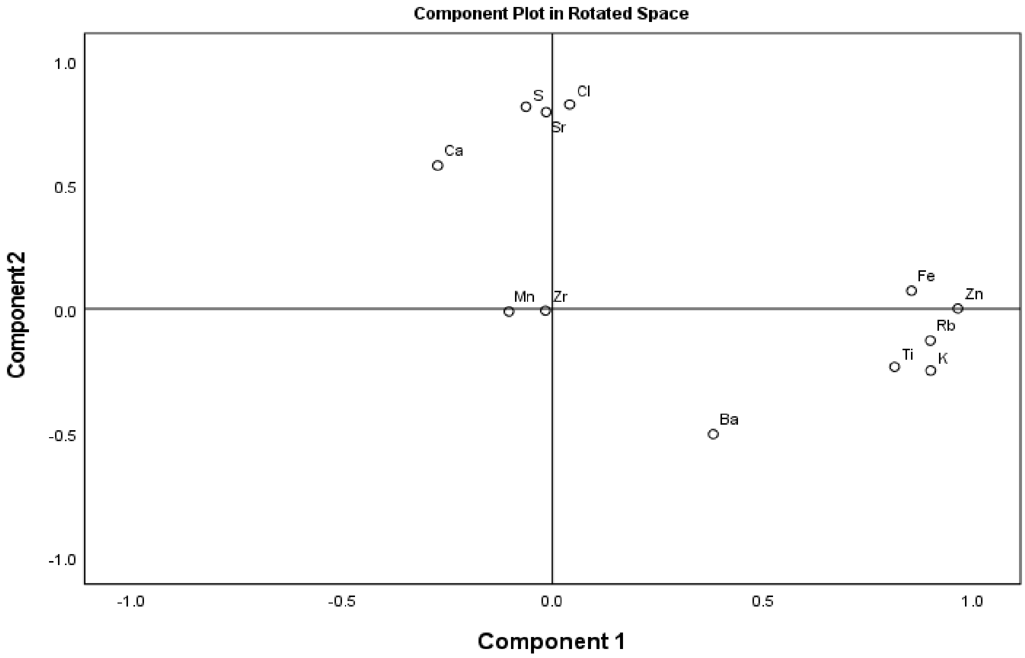

Figure 30 Component plot of elements in rotated space from PCA analysis.

Zr/Rb ratio value is abruptly increased from 3 to 4.5 at the boundary between units B and C (approximately 24.32 m DBS) (Figure 31). The ratio gradually declines to 3 at the top of unit E, from 24.32 to 17.37 m DBS. Zr/Rb ratio is approximately 5 and varies from 3 to 5 in units F to the lower part of unit I (14.70–12.66 m DBS). It gradually decreases from 4 to 2.5 in the upper part of unit I (11.80–7.20 m DBS) (Figure 31).

Ti/Ca is a slight change of 16 at 24.32 m DBS before abruptly declining to 0.5 between 24.50 and 21.00 m DBS (Figure 31). The ratio gradually increases and reaches its maximum of 20 at 19.00-17.37 m DBS. The Ti/Ca is an insignificant change in units F to I (Figure 31).

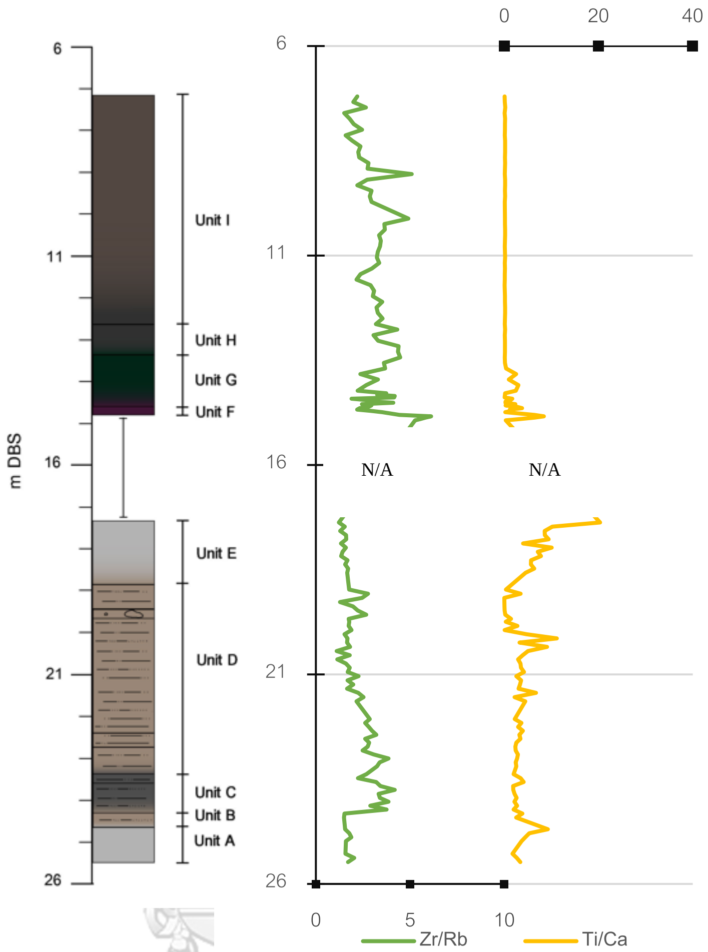

Figure 31 The lithostratigraphic column and variations of Zr/Rb and Ti/Ca ratios of the sediment sequence of the open pit at Samut Sakhon.

4.5 Palynology

Thirty-four pollen taxa can be found in the sediment samples obtained from the pit, divided into 4 assemblages: mangroves, back mangroves, non-mangroves taxa, and unidentified taxa following Santisuk (1983) and Punwong (2007) (Table 7). According to the pollen analysis, the sedimentary sequence can be divided into two main pollen zones, i.e., A and B from the bottom to the top.

Table 7 Pollen assemblage of the sediment sequence of the open pit at Samut Sakhon.

Assemblage	Assemblage name	Plant assemblage
1	mangroves	*Avicennia*, *Bruguiera*, *Lumnitzera*, *Rhizophora*, and *Sonneratia*
2	Back mangroves	*Acanthus*, *Acrostichum*, Combretaceae, *Oncosperma*, *Pandanus*, *Suaeda*, *Stenochlaena*, and *Xylocarpus*
3	Non-mangrove taxa	*Altingia*, Amaranthaceae, Anacardiaceae, Araceae, *Clerodendrum*, *Casuarina*, Cyperaceae, Dipterocapaceae, Fagaceae, *Lagerstroemia*, Magnoliaceae, Myrsinaceae, Myrtaceae, *Pinus*, Poaceae, *Quercus*, Sapindaceae, *Ceratopteris*, *Davillia*, Gleicheniaceae, and *Pteris*
4	Unidentified	-

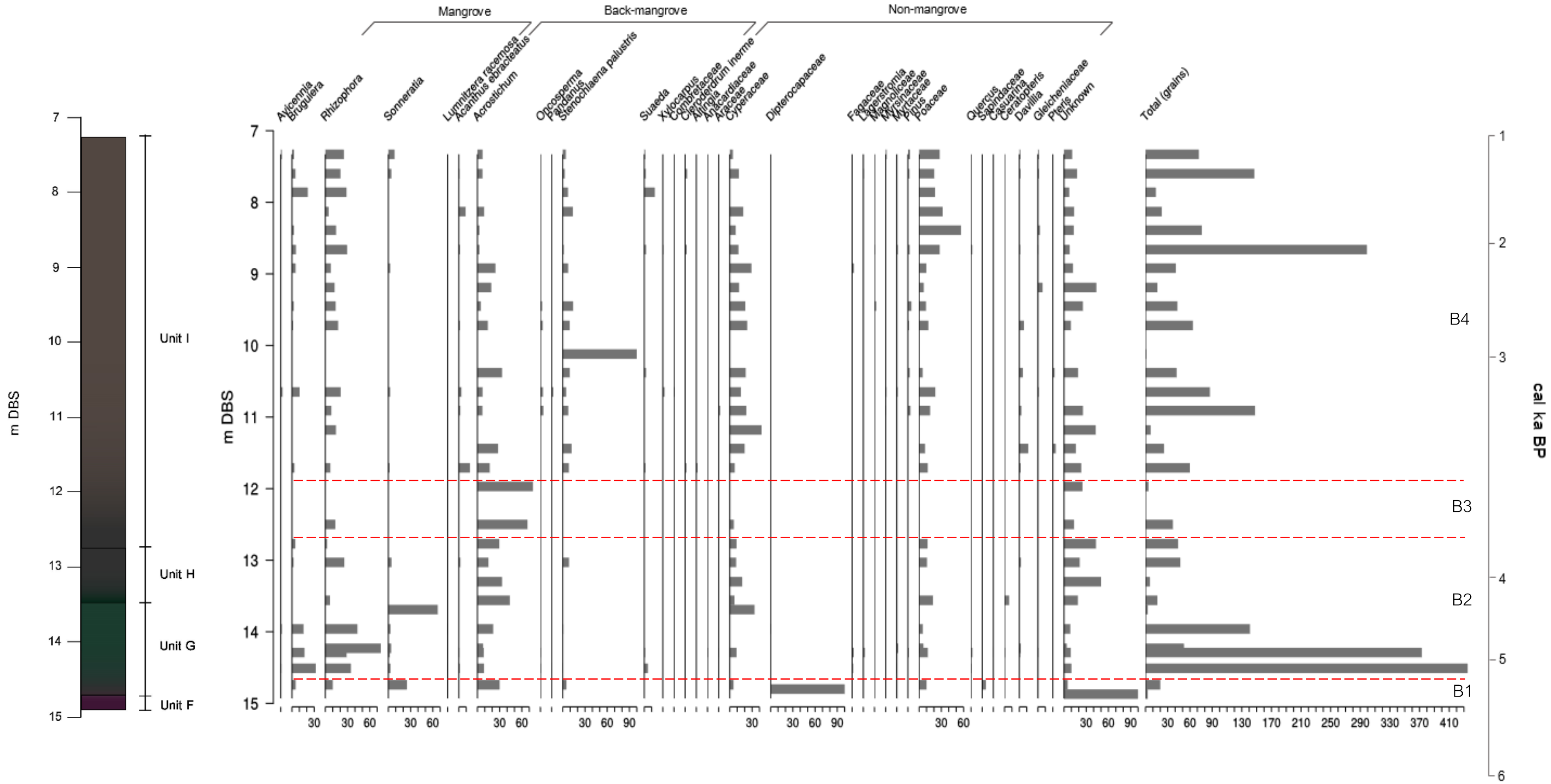

Figure 32 Percentage of pollen assemblage in the sediment sequence of the open pit at Samut Sakhon, red dash shows the boundary of pollen zone.

4.5.1 Pollen zone A (25.48-17.37 m DBS)

The pollen is meager in the pollen zone A, which varies between 2 to 17 pollen grains. Pollens of non-mangrove herb, Amaranthaceae and Poaceae were found in unit A. In unit C, Amaranthaceae pollen significantly increased and reached its maximum of 17 pollen grains. In the middle of unit D, pollen grains are hardly found (< 2 grains and 1 pollen taxon) therefore this interval is defined as the barren zones of pollen. The pollens of *Bruguiera* -landward mangrove plant- and Poaceae are found in unit D. In unit E, two Poaceae pollens are present.

4.5.2 Pollen zone B (14.89 – 7.20 m DBS)

Pollen zone B can be further divided into 4 pollen zones (Figure 32).

4.5.2.1 Pollen zone B1 (14.89-14.70 m DBS)

Pollen zone B1 corresponds to sedimentary unit F. Pollen is abundant in the upper part of pollen zone B1, especially *Acrostichum,* back mangrove pollen taxa, which found 6 grains and reaches 30% (Figure 32). In addition, mangrove pollen taxa, including *Bruguiera*, *Stenochlaena*, *Rhizophora*, and *Sonneratia*, are found in 1, 1, 2, and 5 grains which are 5%, 5%, 10%, and 25%, respectively (Figure 32). Cyperaceae, Poaceae, and Monolete, the non-mangrove pollen taxa, are presented 1-2 grains which are around 5-10% (Figure 32).

4.5.2.2 Pollen zone B2 (14.70-12.66 m DBS)

Pollen zone B2 corresponds to sedimentary units G and H. The mangrove pollen taxa, especially *Bruguiera* and *Rhizophora, Sonneratia* are more abundant than those of the previous pollen zone. However, the percentages of *Bruguiera* and *Rhizophora* decreased by 30-2% and 70-2% from pollen grains of 140 to 1 and 150 to 1, respectively, from the bottom to the top of pollen zone B2. (Figure 32). In contrast, the back-mangrove pollen taxa of *Acrostichum* increased by 2-

39 grains which is 10-40% from the bottom to the top of this pollen zone (Figure 32). Cyperaceae and Poaceae are around 20% at 13.56-13.3 m DBS (Figure 32).

4.5.2.3 Pollen zone B3 (12.60-11.90 m DBS)

Pollen zone B3 corresponds to the lower part of sediment in unit I. *Rhizophora*, mangrove pollen taxa, decreases to 15% which is 5 grains (Figure 32). The back-mangrove pollen taxa of *Acrostichum* became predominant, which is 3-25 grains, around 70-75%. Cyperaceae pollen taxa are found in 5 grains which is 5% at the boundary between pollen zone B2 and B3 (Figure 32).

4.5.2.4 Pollen zone B4 (11.90-7.20 m DBS)

Pollen zone B4 corresponds to sedimentary units I above 11.90 m DBS. This pollen zone found a variety of pollen taxa. Mangrove pollen taxa of *Bruguiera* and *Rhizophora* have been found in 1-16, and 1-88 grains which are around 10-20% and 20-30%, respectively (Figure 32). Back-mangrove pollen taxon of *Acrostichum* significantly decreases compared to the previous zone and continuously declines from 15 to 10% in the pollen zone B4. The non-mangrove pollen taxa have become prevailing (Figure 32). Cyperaceae pollen varies from 3-35 which decreases by 40-20 %, while Poaceae pollen increases 7-83 grains by 15-60% from the bottom to the top of pollen zone B4 (Figure 32).

4.6 Chronology

The chronology of sedimentary succession is based on sequential radiocarbon dating of bulk sediment and marine shells (Table 8). The dating results obtained from the samples in sedimentary units A to E are constrained to the late Pleistocene (Table 8). However, the results derived from the samples in sedimentary units F to I are limited to the mid/late Holocene (Table 8). This abrupt change in dating results indicates a possible unconformity between 18.47 and 14.89 m DBS. Therefore, further analysis is separated into the sections from 25.48 to 18.47 m DBS and from 14.89 to 7.54 m DBS.

The chronology of the lower part of the sedimentary succession (from 25.48 to 18.47 m DBS) relied on the sequential radiocarbon dates of bulk sediments. The dating results obtained from sample no. #10, #9, and #7 are significantly inconsistent with those from the adjacent depth (Table 8). They are excluded from further analysis since the contamination of older or younger origins of organic material in the bulk sediment frequently exceeds the depositional timeframe (Grimm et al., 2009). Consequently, the age-depth model for section 25.48-18.47 m DBS is based on interpolating the dating results from sample no. #11, #8, and #6, extending from 26500 to 22650 cal years BP (Figure 33). The sedimentation rate is c. 0.1 cm/year at c. 25.48-22.06 m DBS, and significant increases to 1.5 cm/yr at c. 22.06-18.47 m DBS (Figure 33).

In the upper part of the sedimentary succession (from 14.89 to 7.54 cm DBS), the chronology extends from 5400 to 1064 cal years BP. In addition, since it was shell samples the calibration will be used of the MARINE20 curve instead. However, the dating results obtained from sample no. #2 does not fit this general pattern and resulted in an older age than expected. This older age is possibly caused by reworking and excluded from the age-depth model constructed by Bacon. The deposition rate is approximately 0.11 cm/year from 13.77 to 14.88 m DBS, 0.92 cm/year from 13.76-11.66 m DBS, and 0.14 cm/year from 11.65-7.20 m DBS hereafter (Figure 34).

Table 8 14C dated from bulk sediment and shell samples for Samut Sakhon site.

Sample no.	m DBS	Material	14C age (BP ± σ)	Cal year BP	Unit
#1	7.54	Shell	1672 ± 24	1,239	I
#2	9.88	Shell	4565 ± 30	4,791	I
#3	11.66	Shell	4070 ± 28	4,156	I
#4	13.78	Shell	4245 ± 29	4,385	G
#5	14.89	Shell	5056 ± 26	5,400	F
#6	18.47	Bulk sediment	18805 ± 75	22,732	E
#7	21.34	Bulk sediment	22415 ± 144	26,384	D
#8	22.06	Bulk sediment	19054 ± 95	22,985	D
#9	23.12	Bulk sediment	29720 ± 172	33,927	D
#10	25.48	Bulk sediment	14305 ± 62	17,116	A
#11	25.50	Bulk sediment	22220 ± 102	26,507	A

Grey stripe represent excluded samples from this study

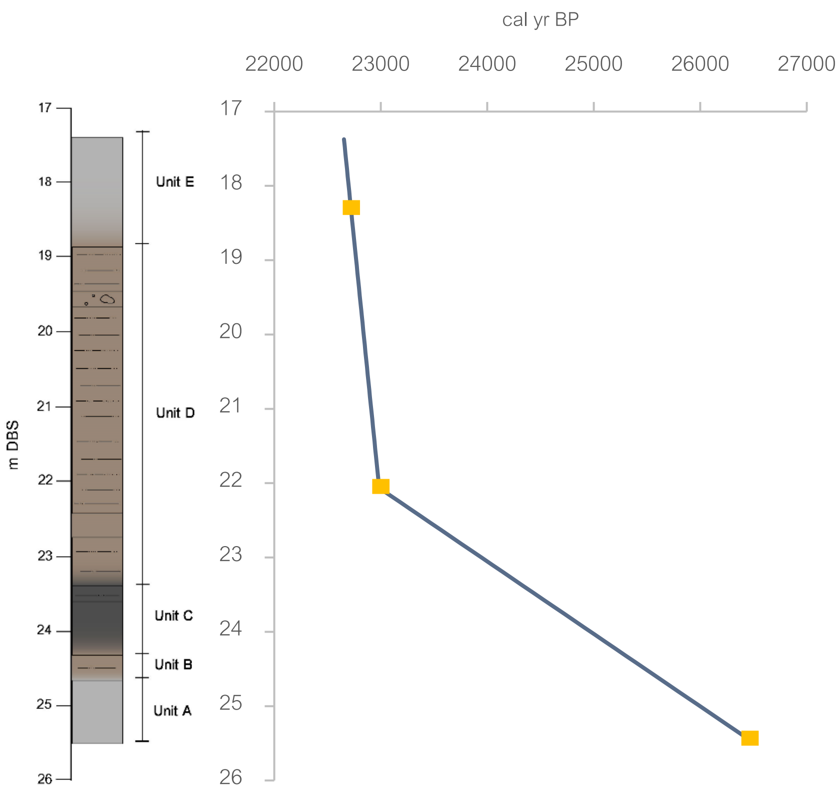

Figure 33 Age-depth relationship curve of sedimentary sequences below the hiatus in the late-Pleistocene, yellow dot show dating result from 25.50, 22.06, and 18.47 m DBS.

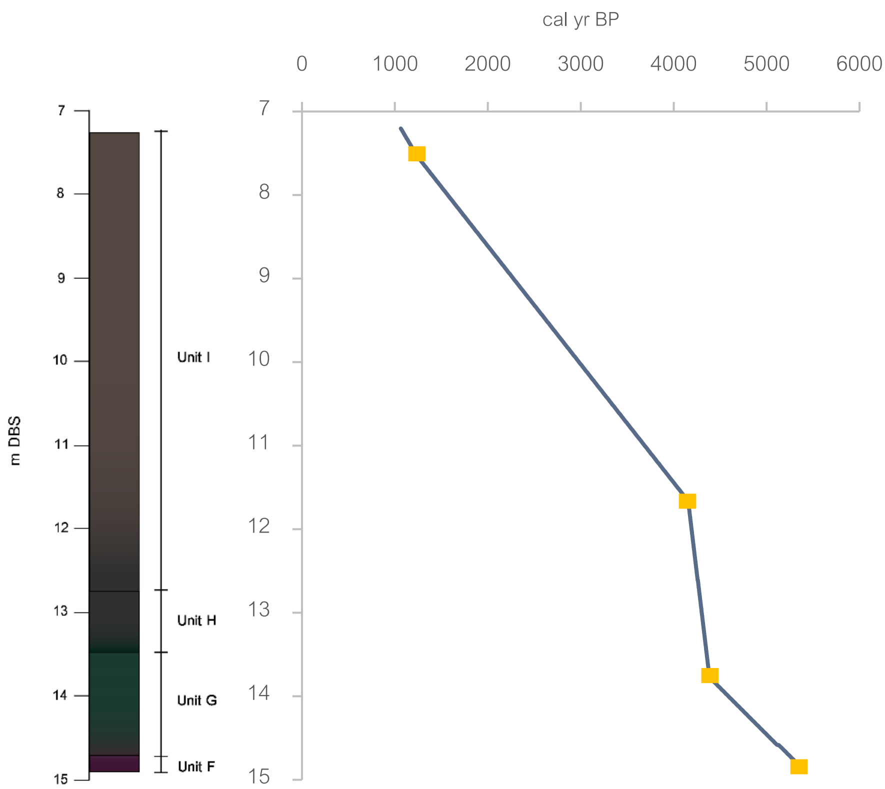

Figure 34 Age-depth relationship curve of sedimentary sequences upper the hiatus in the mid/late Holocene, yellow dot show dating result from 14.89, 13.78, 11.66, and 7.54 m DBS.

CHAPTER 5
DISCUSSION

Regarding sequential radiocarbon dating, the sedimentary sequence at the open pit at Samut Sakhon can be divided into the late Pleistocene approximately 26.5-22.6 cal ka BP and the mid/late Holocene deposits approximately 5.4-1.1 cal ka BP.

5.1 Environmental reconstruction during the late Pleistocene

The radiocarbon dating obtained from sample no. #11, #8, and #6 demonstrated that the sedimentary section was deposited at 26.5-22.7 cal ka BP, which was contemporary with the Last Glacial Maximum (LGM: 25-19 cal ka BP) (e.g., Negri, 2012; Puchala et al., 2011; Gorbarenko et al., 2022) (Table 8). The sea level lowstand during the LGM exposed the Sunda shelf connected the Southeast Asian Mainland to the Indonesian archipelago (e.g., Sathiamurthy & Voris, 2006; Puchala et al., 2011; Rugmai & Grote, 2023). Since, Samut Sakhon was a part of the Sundaland, the sedimentary deposit was potentially controlled by the Tha Chin and Chao Phraya Rivers (Sinsakul, 2000; Tanabe et al., 2003). The reconstructions of the LGM climate generally revealed the strengthening of winter monsoon, making the persistent cooler and drier conditions than present of the Savanna (tropical wet and dry) climate (e.g. van Campo et al., 1982; Huang et al., 1997; Hodell et al., 1998; von Rad et al., 1999; Hope, 2001; Naidu, 2004; Prabhu et al. 2004; White et al., 2004; Tiwari et al., 2006; Ansari and Vink, 2007; Cosford et al., 2010; Fleitmann et al. 2011).

Sedimentary characteristics of this stage include sediment from units A to E that mixed light grey clay and brown/grey clayey silt layer. The paucity of pollen that identifies as a barren zone of pollen is possibly caused by the oxidizing of the study area that agrees with the color of the sediment. These results possibly indicate the temporal exposure of the study area, which was the floodplain of Tha Chin and Chao Phraya Rivers during the LGM at 26.5-23.0 cal ka BP.

Noticeably, the significant increases in sand fraction and volume metric diameter were consistent with relatively low organic matter, regard to LOI550, and high Ti/Ca value in sedimentary unit D at 21.6-19.1 m DBS. These results obviously suggested an abruptly increased runoff intensity in the study area at 23.0-22.8 cal ka BP (Figure 35).

5.2 Environmental Reconstruction during the mid/late Holocene

In the mid-Holocene, sea level increased and reached its highstand at around 8-4 cal year BP (Somboon & Thiramongkol, 1992; Horton et al., 2005; Bird et al., 2010; Li et al., 2012; Hutangkura, 2014; Surakiatchai et al., 2018). However, the timing of the mid-Holocene highstand has been under debate. For example, the reconstruction of the sea level regarding pollen records in Chao Phraya Plain, Thailand, suggested the highstand at 8.4 cal yr BP (Hutangkura, 2014). However, the dating of the peat layer obtained from the same area indicated a highstand of around 7.3-6 year BP (Somboon & Thiramongkol, 1992) that was contemporary with the dating of peat layer at Singapore by Tjia (1996) and Bird et al. (2010). Whereas, Horton et al. (2005) suggest that the sea level high stand was at 4.85 – 4.45 cal year BP. In the late Holocene, the sea level has been generally considered to be a gradual fall based on various studies associated with the glacial isostatic adjustment (GIA) model (Horton et al., 2005; Zong, 2013; Surakiatchai et al., 2018). However, some records suggest that sea levels have been fluctuating after the mid-Holocene highstand (Sinsakul, 1992; Tjia, 1996; Jirapinyakul et al., 2023). Therefore, the low central plain, including the study area, was directly influenced by the marine processes during the mid/late Holocene.

The radiocarbon dating obtained from sample #5, #4, #3, and #1 indicated that the sedimentary section was deposited at 5.4-1.1 cal ka BP (Table 8). Sedimentary characteristics of the mid/late Holocene stage include sedimentary units F to I. The presence of high mangrove pollen taxa in greenish-dark grey clay and dark grey clay approximately 14.9-13.7 m DBS is consistent with relatively high organic content, indicating the influence of marine processes (Figure 36). The high pollen accumulation rate that obtained by calculating pollen grains with the rate of deposition suggested the thriving of mangrove forests in the study area at 5.4-4.4 cal ka BP.

The transformation of sediment from greenish-dark grey clay and dark grey clay to dark brown clayey silt is consistent with the decrease in pollen number associated with lower organic matters, referred to the regression at 4.4-4.2 cal ka BP. Moreover, this interpretation is supported by the occupation of the back-mangrove pollen taxa at 13.6-11.7 m DBS (Figure 36). The environment at this time is likely to be a back-mangrove forest.

Non-mangrove pollen taxa became predominant at 4.2–2.3 cal ka BP. The pollen accumulation rate of Cyperaceae and Poaceae which is non-mangrove pollen assemblage indicates that freshwater has more influence in this area. The value of the Zr/Rb ratio, sand fraction, and volume metric mean diameter slightly increased during this time interval referring to higher transportation environment energy. These results suggest the gradual sea level lowering at 4.2–2.3 cal ka BP and the environment in Samut Sakhon seems to be a wetland (Figure 36).

Organic matter and volume metric mean diameter increased at 8.9-7.2 m DBS, demonstrating the higher transportation energy at 2.3-1.1 cal ka BP (Figure 36). Pollen was abundant, especially Poaceae and *Rhizophora*, at this depth. The high pollen accumulation rates of both mangrove and non-mangrove pollen taxa suggested the sea level again increased together with freshwater influence by an occasional increase in runoff at 2.3-1.1 cal ka BP. The environment seems to transfer from a wetland to a brackish water area in this time interval.

5.3 Unconformity of the sedimentary sequence

The sediment in the Late-Pleistocene to Holocene of Chao Phraya delta is known as Bangkok Clay (Sinsakul, 2000; Tanabe et al., 2003). Bangkok clay consists of soft clay from the Holocene and stiff clay from the Late-Pleistocene that unconformably overlaid (Tanabe et al., 2003). Tanabe et al. (2003) suggested the stratigraphy evolution at Tha Chin and Chao Phraya delta plains that shallow marine and fluvial sediment in the Late Pleistocene unconformably overlaid by basal lag sediment with a sharp erosional surface from the mid-Holocene high stand, this erosional surface may occur due to marine transgression or regression.

The sedimentary sequence data from this study is likely to be consistent with Tanabe et al. (2003). The intervals at 17.3-14.9 m DBS in the open pit in Samut Sakhon are possibly divided by the unconformity. The laminate light grey clay layer in unit E indicates deposition during the Late Pleistocene at approximately 22.7 cal ka BP adjacent to the oxidized purple clay layer in unit F indicates deposition during the mid-Holocene at approximately 5.4 cal ka BP.

5.4 Recommendation

The open pit study site was 4 km distance from Phanom Surin Shipwreck in Samut Sakhon Province. Phanom Surin Shipwreck was 2 m depth of the pond edge and 8 km distance from the Gulf of Thailand, the surrounding area was shrimp farms and mangrove plants (The 1st Regional Office of Fine Arts Department, 2016). The dating result indicates an age of approximately 1.1-1.3 cal ka BP (The 1st Regional Office of Fine Arts Department, 2016).

In this study, shell samples were found at 7.5 m depth below the surface (the surface refers to rural road 2004 level) around the open pit indicating an age of 1.2 cal ka BP which is similar to the age of Phanom Surin Shipwreck. These results possibly show that at around 1.3 cal ka BP when the upper Gulf of Thailand was invaded by marine water. However, the inconsistency in depth between the open pit and shipwreck need to be further studied by the differential global positioning system.

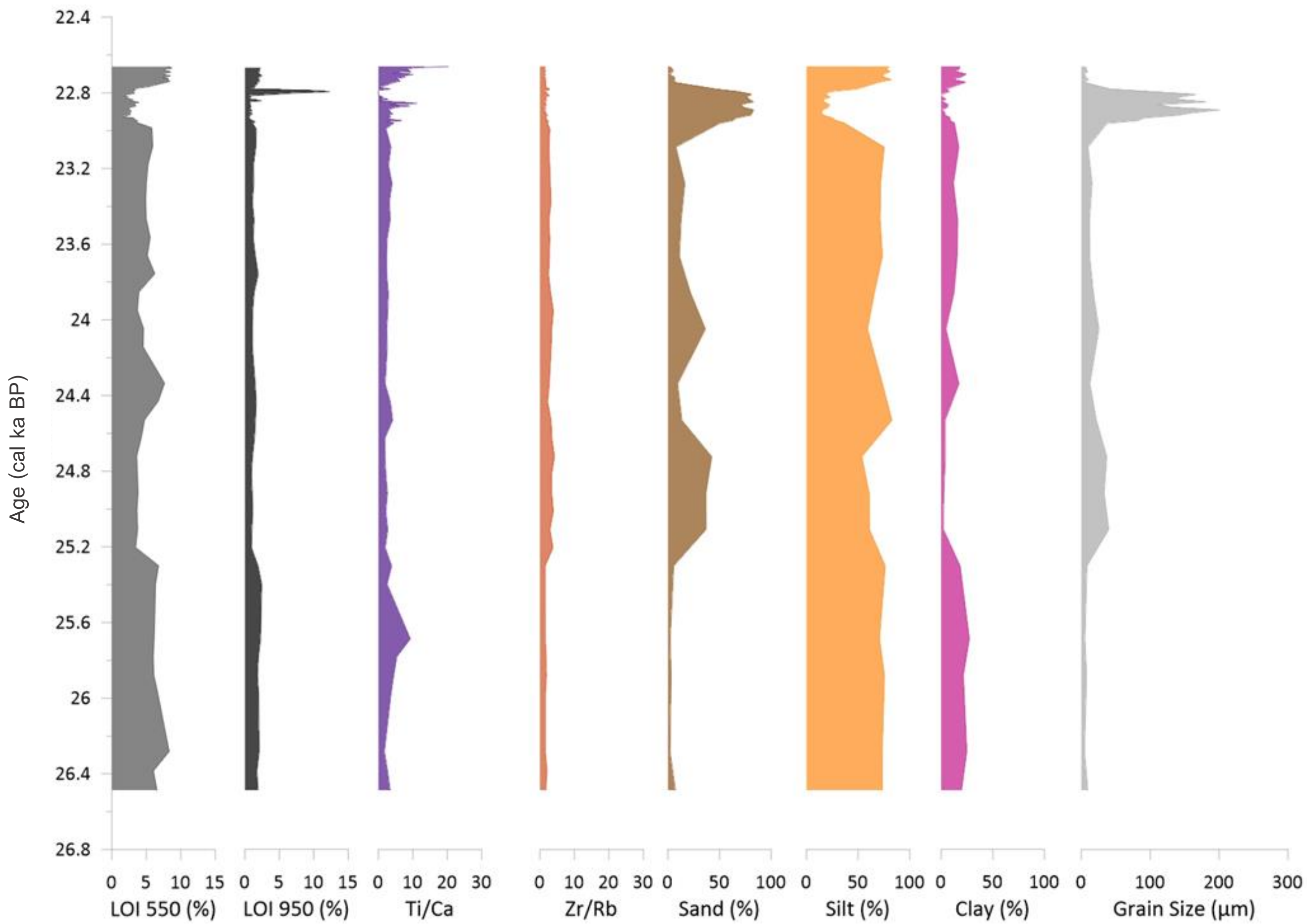

Figure 35 Samut Sakhon evolution in the late Pleistocene according to LOI, Ti/Ca, Zr/Rb, percentage of sand, silt, clay, and grain size.

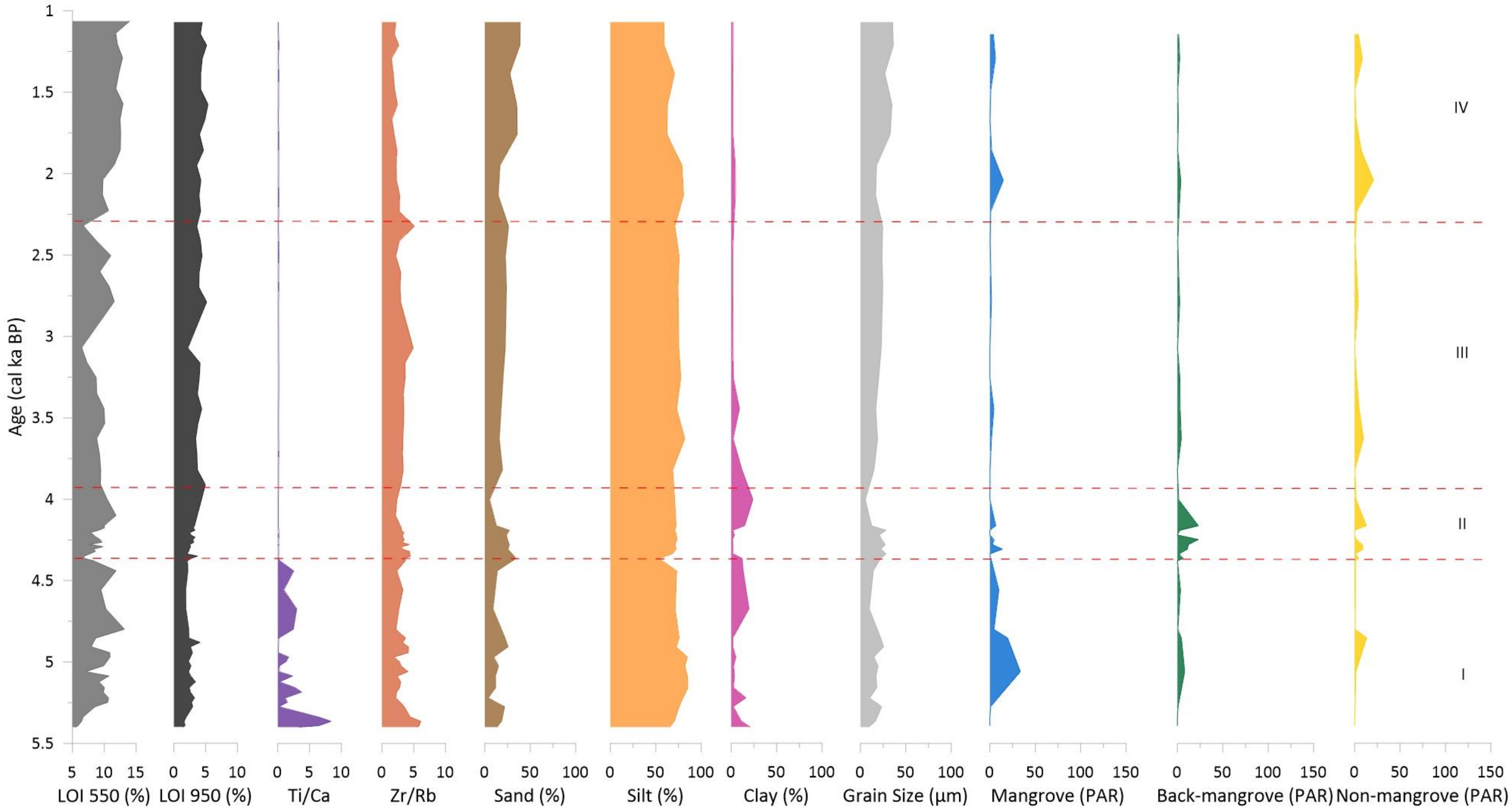

Figure 36 Samut Sakhon evolution 4 stage in the mid/late Holocene according to LOI, Ti/Ca, Zr/Rb, grain size, and mangrove, back-mangrove, and non-mangrove pollen accumulation rate (PAR).

CHAPTER 6
CONCLUSION AND RECOMENDATION

This study uses LOI, Ti/Ca, and Zr/Rb ratio, grain size, and pollen interpretation together with radiocarbon dating to reconstruct past environments and evolution in Samut Sakhon site, the upper Gulf of Thailand. The past environment in Samut Sakhon site can divided into two separate parts including the late Pleistocene and the mid/late Holocene.

In the late Pleistocene, the paucity of pollen possibly indicates the temporal exposure of the study area during a dry condition at 26.5-23.0 cal ka BP. Followed by abruptly increased runoff intensity at 23.0-22.8 cal ka BP.

In the mid to late Holocene, the thriving of mangrove forest communities due to sea level transgression happened at 5.4-4.4 cal ka BP. The mangrove forest was transferred to the back-mangrove forest during sea level regression at 4.4-4.2 cal ka BP, and then the sea level continuously decreased until 2.3 cal ka BP. Subsequently, sea level increased in the study area by approximately 2.3-1.1 cal ka BP together with freshwater influence by an occasional increase in runoff.

The sedimentary sequence in Samut Sakhon shows an unconformity at 17.3-14.9 m DBS. The unconformity present between the laminate light grey clay at the Late-Pleistocene and the oxidized purple clay layer at the mid-Holocene.

The correlation between the open pit study site and the Phanom Surin Shipwreck indicates a similar age of around 1.2-1.3 cal ka BP, suggesting that the open pit has been at a deep point deeper than the Phanom Surin Shipwreck during the late Holocene.

The measurement of the depth of the open pit was only conducted by using an Automatic level where Samut Sakhon Rural Road 2004 was a reference level. For further study, level measurement of an Automatic level and measurement of a Differential Global Positioning System where Mean Sea Level was a reference level should be combined to represent the actual level and can be correlated with another study.

REFERENCES

Alptekin, A., & Hatipoglu, Z. (2018). *ENGINEERING PROPERTIES OF CALICHE*.

Bird, M. I., Austin, W. E., Wurster, C. M., Fifield, L. K., Mojtahid, M., & Sargeant, C. (2010). Punctuated eustatic sea-level rise in the early mid-Holocene [Article]. *Geology*, *38*(9), 803-806. https://doi.org/10.1130/G31066.1

Bird, M. I., Fifield, L. K., Teh, T. S., Chang, C. H., Shirlaw, N., & Lambeck, K. (2007). An inflection in the rate of early mid-Holocene eustatic sea-level rise: A new sea-level curve from Singapore [Article]. *Estuarine, Coastal and Shelf Science*, *71*(3-4), 523-536. https://doi.org/10.1016/j.ecss.2006.07.004

Bowen, D. Q. (2009). Last Glacial Maximum. In V. Gornitz (Ed.), *Encyclopedia of Paleoclimatology and Ancient Environments* (pp. 493-495). Springer Netherlands. https://doi.org/10.1007/978-1-4020-4411-3_122

Chabangborn, A., Punwong, P., Phountong, K., Nudnara, W., Yoojam, N., Sainakum, A., Won-In, K., & Sompongchaiyakul, P. (2020). Environmental changes on the west coast of the Gulf of Thailand during the 8.2 ka event. *Quaternary International*, *536*, 103-113. https://doi.org/10.1016/j.quaint.2019.12.020

Choowong, M. (2002). The geomorphology and assessment of indicators of sea-level changes to study coastal evolution from the Gulf of Thailand. *Proceedings of the Symposium on Geology of Thailand*.

Dusitapirom, U., Choowong, M., & Daorerk, V. (2008). Analysis in genesis and pattern of limestone sea notches from Sam Roi Yot National Park, Phrachuap Kirikhan Province, Southern Thailand. 35 -39.

Geyh, M., Streif, H., & Kudrass, H. (1979). Sea-level changes during the Late Pleistocene and Holocene in the Strait of Malacca. *Nature*, *278*, 441-443. https://doi.org/10.1038/278441a0

Hanebuth, T., Stattegger, K., & Grootes, P. (2000a). Rapid Flooding of the Sunda Shelf: A Late-Glacial Sea-Level Record. *Science (New York, N.Y.)*, *288*, 1033-1035. https://doi.org/10.1126/science.288.5468.1033

Hanebuth, T., Stattegger, K., & Grootes, P. M. (2000b). Rapid Flooding of the Sunda Shelf: A Late-Glacial Sea-Level Record. *Science*, *288*(5468), 1033-1035. https://doi.org/10.1126/science.288.5468.1033

Hesp, A. P., Chang Chew, H., Hilton, M., Chou Loke, M., & Turner, I. M. (1998). A First Tentative Holocene Sea-Level Curve for Singapore. *Journal of Coastal Research*, *14*(1), 308-314. http://www.jstor.org/stable/4298779

Horton, B. P., Gibbard, P. L., Milne, G. M., Morley, R. J., Purintavaragul, C., & Stargardt, J. M. (2005). Holocene sea levels and palaeoenvironments, Malay-Thai Peninsula, southeast Asia [Article]. *Holocene*, *15*(8), 1199-1213. https://doi.org/10.1191/0959683605hl891rp

Hutangkura, T. (2012). *Pollen analysis of the Holocene sedimentary sequences from the Lower Central Plain of Thailand and its implications for understanding palaeoenvironmental and phytogeographical changes.* [History, University of Nice, France].

Hutangkura, T. (2014). A New Interpretation of the Boundary of Dvaravati Shoreline on the Lower Central Plain. *Damrong Journal*, *13*, 11-44.

Jirapinyakul, A., Nudnara, W., Punwong, P., Nohall, R., Englong, A., Phujareanchaiwon, C., Yamoah, K. A., & Choowong, M. (2023). ENSO may have contributed to sea level changes in the Gulf of Thailand during the Late-Holocene. *The Holocene*, 09596836231197745. https://doi.org/10.1177/09596836231197745

Li, Z., Saito, Y., Mao, L., Tamura, T., Li, Z., Song, B., Zhang, Y., Lu, A., Sieng, S., & Li, J. (2012). Mid-Holocene mangrove succession and its response to sea-level change in the upper Mekong River delta, Cambodia. *Quaternary Research*, *78*(2), 386-399. https://doi.org/10.1016/j.yqres.2012.07.001

Nudnara, W. (2019). *Reconstruction of sea level fluctuation and environmental change in Khao Sam Roi Yot National Park, Changwat Prachuap Khiri Khan during the late holocene* (Publication Number 6072092223) Chulalongkorn University]. http://cuir.car.chula.ac.th/handle/123456789/65003

Oliver, G. J. H., & Terry, J. P. (2019). Relative sea-level highstands in Thailand since the Mid-Holocene based on 14C rock oyster chronology. *Palaeogeography, Palaeoclimatology, Palaeoecology*, *517*, 30-38. https://doi.org/https://doi.org/10.1016/j.palaeo.2018.12.005

Plicht, J., Ramsey, C., Heaton, T., Scott, E. M., & Talamo, S. (2020). Recent Developments in Calibration for Archaeological and Environmental Samples. *Radiocarbon*, *62*, 1-23. https://doi.org/10.1017/RDC.2020.22

Sainakum, A., Jittangprasert, P., Sompongchaiyakul, P., & Jirapinyakul, A. (2021). Using n-alkanes as a proxy to reconstruct sea-level changes in Thale Noi, the west coast of the Gulf of Thailand. *Journal of Asian Earth Sciences*, *213*, 104740. https://doi.org/https://doi.org/10.1016/j.jseaes.2021.104740

Santisuk, T. (1983). Taxonomy and distribution of terrestrial trees and shrubs in the mangrove formations in Thailand. In (Vol. 31, pp. 63-91).

Sinsakul, S. (1992). Evidence of quarternary sea level changes in the coastal areas of Thailand: a review. *Journal of Southeast Asian Earth Sciences*, *7*(1), 23-37. https://doi.org/https://doi.org/10.1016/0743-9547(92)90012-Z

Sinsakul, S. (2000). Late Quaternary geology of the Lower Central Plain, Thailand. *Journal of Asian Earth Sciences*, *18*(4), 415-426. https://doi.org/https://doi.org/10.1016/S1367-9120(99)00075-9

Somboon, J. R. P. (1988). Paleontological study of the recent marine sediments in the lower central plain, Thailand. *Journal of Southeast Asian Earth Sciences*, *2*(3), 201-210. https://doi.org/https://doi.org/10.1016/0743-9547(88)90031-1

Somboon, J. R. P. (1990). Palynological study of mangrove and marine sediments of the Gulf of Thailand. *Journal of Southeast Asian Earth Sciences*, *4*(2), 85-97. https://doi.org/https://doi.org/10.1016/0743-9547(90)90008-2

Somboon, J. R. P., & Thiramongkol, N. (1992). Holocene highstand shoreline of the Chao Phraya delta, Thailand. *Journal of Southeast Asian Earth Sciences*, *7*(1), 53-60. https://doi.org/https://doi.org/10.1016/0743-9547(92)90014-3

Southorn, Kashgarian, M., Fontugne, Metivier, & Yim, W. (2002). Marine Reservoir Corrections for the Indian Ocean and Southeast Asia. *Radiocarbon*, *44*, 167-180. https://doi.org/10.1017/S0033822200064778

Surakiatchai, P., Choowong, M., Charusiri, P., Ch, T., Chawchai, S., Pailoplee, S., Jirapinyakul, A., Phantuwongraj, S., Chutakositkanon, V., Kongsen, S., Nimnate, P., & Bissen, R. (2018). Paleogeographic Reconstruction and History of the Sea Level Change at Sam Roi Yot National Park, Gulf of Thailand. *Natural history*, *18*, 112-134.

Tanabe, S., Saito, Y., Sato, Y., Suzuki, Y., Sinsakul, S., Tiyapairach, S., & Chaimanee, N. (2003). Stratigraphy and Holocene evolution of the mud-dominated Chao Phraya delta, Thailand. *Quaternary Science Reviews*, *22*(8), 789-807. https://doi.org/https://doi.org/10.1016/S0277-3791(02)00242-1

The 1st Regional Office of Fine Arts Department, R. (2016). *Preliminary report on the archaeological study of the Phanom Surin Shipwreck 2013-2015*.

Tjia, H. D. (1996). Sea-level changes in the tectonically stable Malay-Thai Peninsula. *Quaternary International*, *31*, 95-101. https://doi.org/https://doi.org/10.1016/1040-6182(95)00025-E

Watson, J. G. (1928). *Mangrove forests of the Malay Peninsula / by J. G. Watson*. Printed by Fraser & Neave.

Zhang, H., Liu, S., Wu, K., Cao, P., Pan, H.-J., Wang, H., Cui, J., Li, J., Khokiattiwong, S., Kornkanitnan, N., & Shi, X. (2022). Evolution of sedimentary environment in the Gulf of Thailand since the last deglaciation. *Quaternary International*, *629*, 36-43. https://doi.org/https://doi.org/10.1016/j.quaint.2021.02.018

Zhang, J., Tomczak, M., Witkowski, A., Zhen, X., & Li, C. (2023). A fossil diatom-based reconstruction of sea-level changes for the Late Pleistocene and Holocene period in the NW South China Sea. *Oceanologia*, *65*(1), 211-229. https://doi.org/https://doi.org/10.1016/j.oceano.2022.05.004

Zong, Y. (2013). SEA-LEVELS, LATE QUATERNARY | Late Quaternary Relative Sea-Level Changes in the Tropics. In S. A. Elias & C. J. Mock (Eds.), *Encyclopedia of*

Quaternary Science (Second Edition) (pp. 495-502). Elsevier.
https://doi.org/https://doi.org/10.1016/B978-0-444-53643-3.00142-4

APPENDICES

APPENDIX A
LOSS ON IGNITION

m DBS	DW105	DW550	DW950	LOI550	LOI950
25.48	2.648	2.475	2.425	6.533	1.888
25.38	3.898	3.663	3.595	6.029	1.744
25.28	2.851	2.614	2.555	8.313	2.069
24.98	2.525	2.357	2.307	6.653	1.980
24.88	2.697	2.533	2.484	6.081	1.817
24.79	2.302	2.164	2.119	5.995	1.955
24.70	2.465	2.314	2.258	6.126	2.272
24.41	2.796	2.619	2.551	6.330	2.432
24.32	3.250	3.030	2.968	6.769	1.908
24.23	2.760	2.665	2.639	3.442	0.942
24.13	3.045	2.931	2.900	3.744	1.018
24.04	2.666	2.569	2.539	3.638	1.125
23.94	2.919	2.808	2.777	3.803	1.062
23.85	2.128	2.049	2.029	3.712	0.940
23.76	2.477	2.388	2.361	3.593	1.090
23.66	3.316	3.175	3.129	4.252	1.387
23.57	2.487	2.369	2.331	4.745	1.528
23.47	2.565	2.393	2.351	6.706	1.637
23.38	2.344	2.165	2.130	7.637	1.493

23.19	3.220	3.074	3.039	4.534	1.087
23.10	2.527	2.411	2.384	4.590	1.068
23.00	2.401	2.312	2.285	3.707	1.125
22.91	2.246	2.158	2.128	3.918	1.336
22.82	2.745	2.574	2.521	6.230	1.931
22.72	2.024	1.920	1.889	5.138	1.532
22.63	1.996	1.885	1.861	5.561	1.202
22.53	2.267	2.154	2.124	4.985	1.323
22.44	2.248	2.138	2.114	4.893	1.068
22.35	2.099	1.994	1.967	5.002	1.286
22.25	2.172	2.058	2.031	5.249	1.243
22.16	1.703	1.602	1.575	5.931	1.585
22.06	2.365	2.228	2.189	5.793	1.649
21.64	1.809	1.746	1.726	3.483	1.106
21.54	1.862	1.792	1.764	3.759	1.504
21.44	2.635	2.548	2.521	3.302	1.025
21.34	3.337	3.229	3.203	3.236	0.779
21.24	1.775	1.748	1.737	1.521	0.620
21.14	2.911	2.844	2.824	2.302	0.687
21.04	2.950	2.870	2.848	2.712	0.746
20.94	2.372	2.311	2.285	2.572	1.096
20.84	2.851	2.771	2.752	2.806	0.666
20.74	2.730	2.657	2.629	2.674	1.026
20.64	2.683	2.616	2.592	2.497	0.895
20.54	2.743	2.675	2.655	2.479	0.729
20.44	2.222	2.146	2.127	3.420	0.855

20.34	2.338	2.258	2.238	3.422	0.855
20.24	2.363	2.289	2.271	3.132	0.762
20.14	2.216	2.129	2.112	3.926	0.767
20.04	2.489	2.429	2.414	2.411	0.603
19.94	1.977	1.916	1.869	3.085	2.377
19.84	2.431	2.388	2.371	1.769	0.699
19.74	2.104	2.053	2.036	2.424	0.808
19.67	1.635	1.608	1.594	1.651	0.856
19.57	1.720	1.683	1.670	2.151	0.756
19.47	1.586	1.534	1.467	3.279	4.224
19.37	2.702	2.622	2.431	2.961	7.069
19.27	2.144	2.072	1.809	3.358	12.267
19.17	2.088	2.021	1.832	3.209	9.052
19.07	2.100	2.021	1.997	3.762	1.143
18.97	2.202	2.086	2.056	5.268	1.362
18.57	3.352	3.070	3.004	8.413	1.969
18.47	3.009	2.765	2.700	8.109	2.160
18.37	4.199	3.856	3.772	8.169	2.000
18.27	3.483	3.229	3.158	7.293	2.038
18.17	4.502	4.121	4.020	8.463	2.243
18.07	2.933	2.710	2.638	7.603	2.455
17.97	3.881	3.586	3.501	7.601	2.190
17.87	4.937	4.514	4.420	8.568	1.904
17.77	3.154	2.913	2.845	7.641	2.156
17.67	3.701	3.415	3.337	7.728	2.108
17.57	4.342	3.963	3.868	8.729	2.188

17.47	3.196	2.938	2.869	8.073	2.159
17.37	3.687	3.411	3.326	7.486	2.305
14.93	3.059	2.908	2.851	4.936	1.863
14.90	4.135	3.911	3.849	5.417	1.499
14.87	3.468	3.265	3.204	5.854	1.759
14.84	2.924	2.736	2.689	6.430	1.607
14.81	3.676	3.431	3.359	6.665	1.959
14.74	3.212	2.938	2.843	8.531	2.958
14.71	2.168	1.940	1.880	10.517	2.768
14.68	2.834	2.532	2.440	10.656	3.246
14.64	3.744	3.376	3.279	9.829	2.591
14.61	3.135	2.821	2.745	10.016	2.424
14.58	3.454	3.137	3.020	9.178	3.387
14.55	2.986	2.666	2.587	10.717	2.646
14.52	3.758	3.493	3.406	7.052	2.315
14.48	3.192	2.876	2.790	9.900	2.694
14.45	3.461	3.101	3.022	10.402	2.283
14.42	1.993	1.776	1.724	10.888	2.609
14.39	4.079	3.637	3.518	10.836	2.917
14.35	3.720	3.425	3.328	7.930	2.608
14.32	3.876	3.555	3.396	8.282	4.102
14.29	3.150	2.877	2.803	8.667	2.349
14.23	2.699	2.344	2.281	13.153	2.334
14.09	3.554	3.191	3.124	10.214	1.885
13.96	3.221	2.916	2.856	9.469	1.863
13.83	4.070	3.588	3.499	11.843	2.187

13.70	2.578	2.365	2.310	8.262	2.133
13.56	3.288	3.065	2.976	6.782	2.707
13.43	3.330	3.102	2.978	6.847	3.724
13.30	3.042	2.806	2.743	7.758	2.071
13.17	3.643	3.330	3.246	8.592	2.306
13.03	3.010	2.759	2.686	8.339	2.425
12.90	3.509	3.165	3.073	9.803	2.622
12.77	3.358	3.099	3.015	7.713	2.501
12.64	3.698	3.342	3.227	9.627	3.110
12.50	3.210	2.912	2.816	9.283	2.991
12.37	2.758	2.518	2.426	8.702	3.336
12.24	3.979	3.649	3.542	8.294	2.689
12.11	3.832	3.532	3.436	7.829	2.505
11.97	3.043	2.764	2.663	9.169	3.319
11.84	3.644	3.279	3.168	10.016	3.046
11.71	2.436	2.193	2.114	9.975	3.243
11.58	3.942	3.476	3.332	11.821	3.653
11.44	3.024	2.708	2.577	10.450	4.332
11.31	2.537	2.299	2.174	9.381	4.927
11.18	3.708	3.359	3.222	9.412	3.695
11.05	3.538	3.211	3.083	9.243	3.618
10.91	3.218	2.935	2.825	8.794	3.418
10.78	3.373	3.034	2.907	10.050	3.765
10.65	3.548	3.195	3.040	9.949	4.369
10.52	3.053	2.784	2.671	8.811	3.701
10.38	3.515	3.209	3.069	8.706	3.983

10.25	2.945	2.731	2.610	7.267	4.109
10.12	3.601	3.369	3.290	6.443	2.194
9.72	3.255	2.879	2.712	11.551	5.131
9.59	3.091	2.758	2.637	10.773	3.915
9.46	3.349	3.038	2.905	9.286	3.971
9.32	2.794	2.486	2.363	11.024	4.402
9.19	3.422	3.124	2.981	8.708	4.179
9.06	3.307	3.086	2.967	6.683	3.598
8.93	2.694	2.407	2.294	10.653	4.195
8.79	2.736	2.471	2.363	9.686	3.947
8.66	2.855	2.576	2.455	9.772	4.238
8.53	3.173	2.806	2.692	11.566	3.593
8.40	2.456	2.149	2.035	12.500	4.642
8.26	3.051	2.668	2.545	12.553	4.031
8.13	3.223	2.821	2.664	12.473	4.871
8.00	3.272	2.849	2.674	12.928	5.348
7.87	2.939	2.592	2.468	11.807	4.219
7.73	3.127	2.743	2.611	12.280	4.221
7.60	2.878	2.508	2.380	12.856	4.448
7.47	2.382	2.095	1.973	12.049	5.122
7.34	2.977	2.626	2.502	11.790	4.165
7.20	2.837	2.440	2.314	13.994	4.441

APPENDIX B

GRAIN SIZE ANALYSIS DATA

Sample no.	m DBS	Volumetric Mean (μm)	% sand	% silt	% clay
10_1	25.48	9.27	7.20	73.13	19.67
30_1	25.28	4.49	2.06	73.25	24.69
70_1	24.88	7.45	3.16	75.43	21.41
90_1	24.70	5.08	2.24	70.55	27.21
130_1	24.32	8.14	5.59	76.12	18.29
150_1	24.13	39.71	36.86	60.94	2.20
170_1	23.94	32.91	36.78	60.66	2.56
190_1	23.76	36.89	42.39	53.58	4.03
210_1	23.57	21.76	13.52	82.62	3.86
230_1	23.38	12.29	9.40	73.44	17.16
260_1	23.10	25.41	36.28	59.06	4.66
280_1	22.91	17.25	21.90	65.66	12.44
300_1	22.72	12.00	11.14	73.42	15.44
320_1	22.53	11.69	12.78	71.23	15.99
340_1	22.35	15.46	16.41	71.66	11.93
360_1	22.16	9.57	7.76	75.18	17.06
520_1	21.64	37.65	50.27	36.87	12.86
540_1	21.44	82.22	62.68	28.80	8.52
560_1	21.24	90.91	66.42	24.57	9.01
580_1	21.04	139.93	80.09	16.39	3.52
600_1	20.84	162.31	81.62	14.77	3.60
620_1	20.64	200.52	82.98	16.10	0.92

640_1	20.44	131.09	72.56	21.14	6.29
660_1	20.24	109.99	70.68	22.49	6.83
680_1	20.04	180.90	82.73	16.26	1.02
700_1	19.84	138.52	78.21	17.12	4.67
700B_1	19.67	143.04	76.07	23.05	0.88
720_1	19.47	166.25	81.03	18.09	0.88
740_1	19.27	104.14	68.22	23.65	8.12
760_1	19.07	41.34	45.98	48.75	5.27
790_1	18.57	4.79	6.37	69.93	23.70
810_1	18.37	10.65	6.63	82.21	11.15
830_1	18.17	6.38	6.45	74.29	19.26
850_1	17.97	4.38	1.56	74.33	24.10
870_1	17.77	9.22	5.21	80.56	14.24
890_1	17.57	6.94	4.48	77.84	17.68
910_1	17.37	6.28	1.73	80.44	17.83
950_1	14.90	9.22	13.45	65.44	21.11
970_1	14.84	16.48	18.48	70.30	11.22
1000_1	14.74	23.31	21.81	75.70	2.48
1020_1	14.68	10.27	3.98	79.81	16.21
1040_1	14.61	17.98	11.97	85.29	2.74
1060_1	14.55	17.10	11.72	84.76	3.52
1080_1	14.48	19.37	15.15	81.95	2.89
1100_1	14.42	14.78	9.99	84.81	5.20
1120_1	14.35	25.42	25.66	72.51	1.83
1140_1	14.29	22.33	22.33	75.80	1.87
1170_1	14.09	9.77	9.09	71.36	19.54

1190_1	13.83	14.11	13.77	73.03	13.20
1210_1	13.56	22.21	34.28	53.69	12.03
1230_1	13.30	28.20	30.12	67.89	1.98
1250_1	13.03	22.66	25.51	72.53	1.97
1270_1	12.77	27.37	26.95	71.22	1.83
1290_1	12.50	23.45	24.95	73.42	1.63
1310_1	12.24	20.74	23.67	72.73	3.60
1330_1	11.97	28.06	27.07	70.81	2.12
1350_1	11.71	12.31	12.80	72.40	14.80
1370_1	11.44	5.30	5.35	70.82	23.82
1390_1	11.18	14.96	19.48	68.67	11.85
1410_1	10.91	18.83	15.91	81.86	2.23
1430_1	10.65	16.79	17.92	72.93	9.15
1450_1	10.38	20.00	20.06	77.49	2.45
1470_1	10.12	22.81	22.48	75.39	2.12
1510_1	9.59	24.53	23.83	74.45	1.72
1530_1	9.32	23.73	22.62	75.72	1.66
1550_1	9.06	24.44	26.16	71.02	2.82
1570_1	8.79	16.69	14.80	80.53	4.67
1590_1	8.53	17.67	16.70	78.77	4.53
1610_1	8.26	32.61	35.59	62.40	2.01
1630_1	8.00	34.61	35.09	62.92	1.99
1650_1	7.73	26.82	27.58	70.68	1.74
1670_1	7.47	36.16	38.53	59.28	2.19
1690_1	7.20	35.27	38.98	58.86	2.16

APPENDIX C

X-RAY FLUORESCENCE DATA

m DBS	Fe (ppm)	Cl (ppm)	K (ppm)	Ca (ppm)	S (ppm)	Ti (ppm)	Mn (ppm)	Ba (ppm)	Zr (ppm)	Sr (ppm)	Rb (ppm)	Zn (ppm)
25.48	27670	10149	14356	1255	163	4256	83	308	271	92	159	52
25.38	34561	11341	13286	1412	276	3728	1184	384	300	125	147	58
25.28	32432	28594	13236	2307	240	3961	177	362	257	109	164	53
24.98	28847	8036	14693	1197	175	4381	111	340	254	77	159	49
24.88	29577	6732	12667	857	186	3805	126	365	286	64	152	47
24.79	27531	7618	13892	751	194	3980	250	358	293	101	165	49
24.70	37705	7820	13657	442	268	4085	406	397	241	72	155	50
24.41	44142	13157	16917	1813	195	4566	331	370	252	91	169	83
24.32	78983	19135	16434	1140	253	4378	1502	407	234	91	154	88
24.23	13828	5587	12788	1545	0	3040	0	374	435	92	116	47

24.13	18485	4482	14180	1342	209	3636	49	374	369	95	128	56
24.04	28835	5058	14259	1567	0	3349	115	376	459	93	119	61
23.94	25093	4666	14316	1354	0	3542	255	401	428	111	126	55
23.85	26533	5156	14356	1655	156	3572	123	453	416	106	125	55
23.76	30953	9025	13445	1676	263	3169	221	389	502	104	120	57
23.66	21235	15589	13381	1789	0	3316	69	352	404	110	118	50
23.57	16421	9481	11169	964	0	3970	28	351	432	90	135	40
23.47	27145	15280	11763	1181	0	4104	120	300	330	69	148	51
23.38	31898	24959	11346	2016	0	3958	160	260	367	99	137	48
23.19	18689	20286	14275	1225	0	3133	99	375	425	111	131	51
23.10	20822	17289	13527	1289	218	3116	135	413	434	102	128	47
23.00	30072	7676	13815	1252	0	3411	142	416	467	107	121	58
22.91	38570	5957	15541	1308	184	3771	267	387	415	96	135	69
22.82	39309	23009	15612	1684	0	4035	167	401	352	99	142	70
22.72	34981	9456	16038	1784	204	4186	134	441	391	104	142	71
22.63	38832	11924	15078	1623	0	4126	185	410	385	100	136	79

22.53	32872	9642	15658	1172	0	4023	158	446	353	115	135	70
22.44	27750	16246	14525	1091	152	3468	123	331	398	92	124	57
22.35	54151	7931	16316	1044	0	4120	519	429	426	92	143	73
22.25	39822	10912	15447	1343	0	3910	326	515	362	88	129	65
22.16	50740	11194	16323	1335	171	4838	328	427	324	106	124	83
22.06	28564	19600	14910	1813	0	4005	74	422	372	107	130	67
21.64	25357	13159	12571	512	0	2282	1939	403	261	97	121	35
21.54	40395	8004	11670	1116	169	2437	1264	320	278	62	110	36
21.44	34670	6732	13654	403	0	2707	113	302	250	54	111	38
21.34	26814	9246	12373	674	225	2042	2685	361	169	80	102	27
21.24	11747	10517	10225	556	0	1851	2040	579	173	61	87	22
21.14	22962	9243	9410	489	0	1750	108	346	161	49	96	22
21.04	17904	6712	10412	631	200	1607	520	295	211	52	93	16
20.94	21595	8863	9891	413	268	1733	9149	662	157	200	93	25
20.84	16526	7514	10189	488	175	1731	667	306	180	56	100	16
20.74	29967	9308	10643	402	376	1377	11638	455	155	205	97	26

20.64	26100	8326	11240	472	246	1377	1659	360	117	63	103	22
20.54	28906	7668	11163	452	232	1767	363	331	173	50	96	23
20.44	30059	11782	11173	287	308	1447	18522	352	119	252	108	26
20.34	35582	20635	9396	156	538	1418	15249	333	162	165	89	24
20.24	17928	13893	10360	507	260	1644	0	349	172	52	104	16
20.14	20915	14281	11140	163	266	1817	97	364	176	56	105	21
20.04	21985	10534	10055	258	411	1218	1551	358	143	59	94	21
19.94	22306	10480	8515	20773	353	1202	8076	351	172	129	91	21
19.84	24479	4395	11212	412	311	1151	505	303	169	42	97	16
19.74	21578	5067	10392	4831	379	1389	3037	349	170	114	96	20
19.67	21264	5023	9941	913	0	1295	47	283	153	51	88	19
19.57	20382	5189	9222	6838	184	1437	1127	335	238	85	89	22
19.47	27657	4710	12640	21261	252	1653	5771	377	216	164	97	29
19.37	22336	4883	10028	53949	0	1786	0	296	185	72	94	23
19.27	15097	4015	9306	142532	187	2095	1235	367	152	94	119	35
19.17	17061	3872	8827	82871	0	1235	891	220	135	140	55	25

19.07	28109	4776	11176	608	0	2111	321	289	249	66	90	38
18.97	31396	5727	11480	7168	216	2346	3147	331	171	121	97	47
18.57	50787	8426	15041	832	0	3755	1556	349	221	111	133	73
18.47	57804	5859	16765	746	276	4733	2101	388	244	105	142	86
18.37	45295	6881	16124	757	204	4266	227	329	222	80	143	74
18.27	41987	2648	16515	788	0	4463	195	379	247	85	147	84
18.17	66127	5068	17763	641	0	4990	5334	427	203	120	151	105
18.07	51307	3505	16914	677	0	4806	346	333	222	96	157	91
17.97	43597	2815	16953	479	0	4819	4165	509	251	148	157	89
17.87	58270	6195	18019	1165	0	4635	564	345	199	76	149	94
17.77	44425	3977	17484	506	0	4769	525	420	255	89	158	92
17.67	42943	3758	17188	567	0	4870	1581	390	245	99	153	82
17.57	35860	5008	17521	564	0	4826	92	368	219	94	170	79
17.47	46134	4380	17470	477	0	4859	410	395	244	78	159	87
17.37	53555	3231	19059	256	0	5205	344	390	198	90	162	92
14.93	20462	3635	6363	12369	2960	3653	192	282	421	90	80	28

14.90	18374	5370	6001	1201	2441	4006	49	278	438	37	79	24
14.87	21320	7400	6017	648	2248	4186	140	259	448	40	77	31
14.84	19136	7879	5646	473	2568	3967	284	216	477	43	78	26
14.81	17285	7961	7607	603	4211	3832	158	245	399	42	90	34
14.74	31715	13751	10383	13746	9527	2643	994	328	359	116	102	42
14.71	31533	8856	10617	2380	10335	3596	262	297	348	80	119	36
14.68	34745	11318	11516	3371	12186	3931	912	321	267	109	122	57
14.64	27917	6918	10616	925	6512	3474	216	326	279	64	120	50
14.61	31637	10696	11104	1261	9563	3462	265	334	321	74	115	43
14.58	31363	14100	11269	11638	8899	3123	513	263	327	136	111	43
14.55	30763	10112	10680	1407	9519	3309	163	348	279	72	114	50
14.52	27773	7457	10158	11446	7433	2566	555	342	386	121	94	37
14.48	30937	8792	10672	11659	7330	3271	504	288	322	143	107	50
14.45	27847	11616	10539	2771	9365	3711	63	294	319	77	116	49
14.42	37286	10433	12419	2428	7461	4121	593	322	246	97	130	63
14.39	23569	16600	9471	27860	4776	2226	497	299	382	180	92	36

14.35	27359	12777	10704	24510	3966	2534	542	291	406	215	97	38
14.32	27073	21807	9959	20164	11959	2454	415	236	332	151	102	45
14.29	27520	12706	10716	16501	3891	2618	448	290	389	155	104	43
14.23	29660	23070	10635	1529	11606	3740	649	307	268	93	121	51
14.09	25411	14056	10204	1076	4530	3202	191	313	302	69	113	46
13.96	26801	12217	10409	3233	8496	3078	138	285	356	83	108	41
13.83	29810	18666	10508	1335	9539	3354	308	279	278	73	118	47
13.70	29113	14111	10196	8052	8695	2950	268	362	386	88	105	40
13.56	25326	10122	10357	17781	2956	2514	404	274	343	121	95	36
13.43	23791	18350	10210	19893	4376	2300	467	273	430	192	96	36
13.30	24282	12978	10466	18061	4072	2473	442	383	401	158	92	32
13.17	25557	18011	10411	17057	5872	2455	405	311	426	190	97	34
13.03	28568	12634	10799	17373	7841	2573	523	302	334	156	101	42
12.90	28063	18135	10643	24319	6016	2492	514	256	315	186	103	39
12.77	26622	12937	10001	14503	3039	2534	391	344	415	158	96	39
12.64	25623	22317	10171	22268	4756	2449	443	330	331	172	104	36

12.50	26243	19290	10605	18782	8677	2741	419	264	361	156	102	35
12.37	28006	19295	11204	16676	5527	2709	468	252	375	158	114	41
12.24	27074	14083	10311	15220	4790	2506	425	253	319	134	99	40
12.11	29080	10875	10917	19049	4866	2691	483	265	363	178	103	40
11.97	30797	17492	11502	18855	5724	2823	573	264	326	194	108	44
11.84	26758	19879	11142	23185	5929	2697	441	323	337	192	109	44
11.71	28969	15914	11506	38259	17535	2775	525	312	311	269	107	51
11.58	36077	20887	11808	34789	9806	2917	639	340	265	233	123	56
11.44	36460	26627	12521	36332	6272	3081	724	273	265	279	112	50
11.31	28056	31416	10755	20596	8181	2452	462	261	315	195	106	46
11.18	27372	26029	10444	21553	13068	2519	493	266	333	168	99	41
11.05	28367	24021	10770	16250	6205	2608	452	243	340	159	105	41
10.91	28486	16217	10590	20008	5266	2595	547	313	352	167	107	45
10.78	27545	28242	10423	22970	6280	2475	546	315	351	186	103	41
10.65	25733	27209	10408	20968	7846	2462	480	274	348	152	101	38
10.52	30073	21339	11392	16988	6197	2605	582	278	349	161	104	42

10.38	27047	25464	10255	15958	6405	2463	515	301	388	151	106	43
10.25	29122	16079	10504	17676	9855	2607	529	294	378	159	104	38
10.12	24809	9604	9610	17983	3296	2362	521	298	452	173	92	39
9.72	28945	42454	9894	21094	8643	2399	583	309	316	208	107	45
9.59	31770	28584	10564	15434	9638	2527	483	278	318	171	111	44
9.46	29090	23861	9868	20148	9817	2400	577	254	307	169	104	42
9.32	31193	40230	10479	14956	6793	2567	612	316	255	168	116	44
9.19	32741	19087	11485	16871	6193	2588	603	281	305	162	112	51
9.06	24016	11518	10138	26280	4680	2377	422	285	453	284	89	35
8.93	33612	35128	11638	20553	10583	2942	571	286	313	185	114	52
8.79	33846	32168	11879	15632	5005	2744	755	294	330	156	118	52
8.66	31637	29904	11620	19963	11771	2566	628	256	265	176	115	48
8.53	34917	27132	12484	19426	11544	2950	690	252	272	158	121	53
8.40	34508	42563	11768	17716	16261	2724	595	316	294	162	124	57
8.26	36458	35968	12414	18115	12433	2961	749	323	248	157	128	53
8.13	31457	40058	11395	29785	31105	2565	511	298	199	185	126	47

8.00	33266	48623	11016	21178	12522	2640	764	296	289	182	118	52
7.87	34142	42067	11492	21480	9954	2800	786	241	247	176	123	52
7.73	34178	51053	11704	15578	9854	2786	618	272	224	171	125	63
7.60	32532	79904	10791	32808	8308	2553	859	261	194	181	129	51
7.47	32331	35380	11304	13210	5580	2627	698	278	308	145	116	48
7.34	33815	44446	11781	27805	30882	2671	657	303	238	206	120	51
7.20	33038	38110	11454	34336	13420	2653	671	306	253	258	115	54

APPENDIX D
RATIOS OF Ti/Ca AND Zr/Rb DATA

m DBS	Ti/Ca	Zr/Rb	m DBS	Ti/Ca	Zr/Rb
25.48	3.39	1.70	14.93	0.30	5.26
25.38	2.64	2.04	14.90	3.34	5.54
25.28	1.72	1.57	14.87	6.46	5.82
24.98	3.66	1.60	14.84	8.39	6.12
24.88	4.44	1.88	14.81	6.35	4.43
24.79	5.30	1.78	14.74	0.19	3.52
24.70	9.24	1.55	14.71	1.51	2.92
24.41	2.52	1.49	14.68	1.17	2.19
24.32	3.84	1.52	14.64	3.76	2.33
24.23	1.97	3.75	14.61	2.75	2.79
24.13	2.71	2.88	14.58	0.27	2.95
24.04	2.14	3.86	14.55	2.35	2.45
23.94	2.62	3.40	14.52	0.22	4.11
23.85	2.16	3.33	14.48	0.28	3.01
23.76	1.89	4.18	14.45	1.34	2.75
23.66	1.85	3.42	14.42	1.70	1.89
23.57	4.12	3.20	14.39	0.08	4.15
23.47	3.48	2.23	14.35	0.10	4.19
23.38	1.96	2.68	14.32	0.12	3.25
23.19	2.56	3.24	14.29	0.16	3.74
23.10	2.42	3.39	14.23	2.45	2.21
23.00	2.72	3.86	14.09	2.98	2.67

22.91	2.88	3.07	13.96	0.95	3.30
22.82	2.40	2.48	13.83	2.51	2.36
22.72	2.35	2.75	13.70	0.37	3.68
22.63	2.54	2.83	13.56	0.14	3.61
22.53	3.43	2.61	13.43	0.12	4.48
22.44	3.18	3.21	13.30	0.14	4.36
22.35	3.95	2.98	13.17	0.14	4.39
22.25	2.91	2.81	13.03	0.15	3.31
22.16	3.62	2.61	12.90	0.10	3.06
22.06	2.21	2.86	12.77	0.17	4.32
21.64	4.46	2.16	12.64	0.11	3.18
21.54	2.18	2.53	12.50	0.15	3.54
21.44	6.72	2.25	12.37	0.16	3.29
21.34	3.03	1.66	12.24	0.16	3.22
21.24	3.33	1.99	12.11	0.14	3.52
21.14	3.58	1.68	11.97	0.15	3.02
21.04	2.55	2.27	11.84	0.12	3.09
20.94	4.20	1.69	11.71	0.07	2.91
20.84	3.55	1.80	11.58	0.08	2.15
20.74	3.43	1.60	11.44	0.08	2.37
20.64	2.92	1.14	11.31	0.12	2.97
20.54	3.91	1.80	11.18	0.12	3.36
20.44	5.04	1.10	11.05	0.16	3.24
20.34	9.09	1.82	10.91	0.13	3.29
20.24	3.24	1.65	10.78	0.11	3.41
20.14	11.15	1.68	10.65	0.12	3.45

20.04	4.72	1.52	10.52	0.15	3.36
19.94	0.06	1.89	10.38	0.15	3.66
19.84	2.79	1.74	10.25	0.15	3.63
19.74	0.29	1.77	10.12	0.13	4.91
19.67	1.42	1.74	9.72	0.11	2.95
19.57	0.21	2.67	9.59	0.16	2.86
19.47	0.08	2.23	9.46	0.12	2.95
19.37	0.03	1.97	9.32	0.17	2.20
19.27	0.01	1.28	9.19	0.15	2.72
19.17	0.01	2.45	9.06	0.09	5.09
19.07	3.47	2.77	8.93	0.14	2.75
18.97	0.33	1.76	8.79	0.18	2.80
18.57	4.51	1.66	8.66	0.13	2.30
18.47	6.34	1.72	8.53	0.15	2.25
18.37	5.64	1.55	8.40	0.15	2.37
18.27	5.66	1.68	8.26	0.16	1.94
18.17	7.78	1.34	8.13	0.09	1.58
18.07	7.10	1.41	8.00	0.12	2.45
17.97	10.06	1.60	7.87	0.13	2.01
17.87	3.98	1.34	7.73	0.18	1.79
17.77	9.42	1.61	7.60	0.08	1.50
17.67	8.59	1.60	7.47	0.20	2.66
17.57	8.56	1.29	7.34	0.10	1.98
17.47	10.19	1.53	7.20	0.08	2.20
17.37	20.33	1.22			

APPENDIX E
PALYNOLOGY

Figure 37 *Bruguiera*

Figure 38 *Rhizophora*

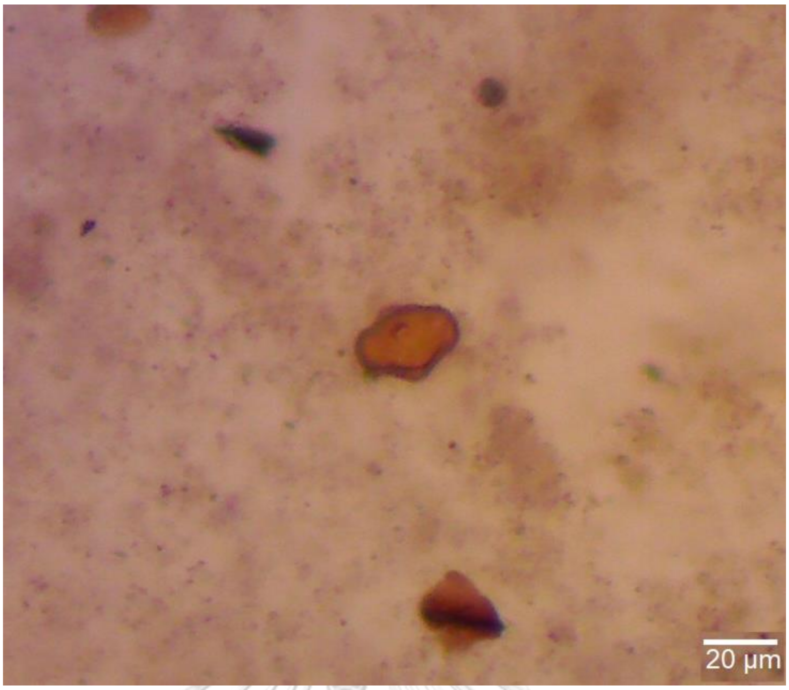

Figure 39 *Sonneratia*

Figure 40 *Stenochlaena*

Figure 41 *Acrostichum*

Figure 42 *Acanthus*

Figure 43 *Suaeda*

Figure 44 *Xylocarpus*

Figure 45 Poaceae

Figure 46 Cyperaceae

Figure 47 *Ceratopteris*

Figure 48 Gleicheniaceae

Figure 49 *Pinus*

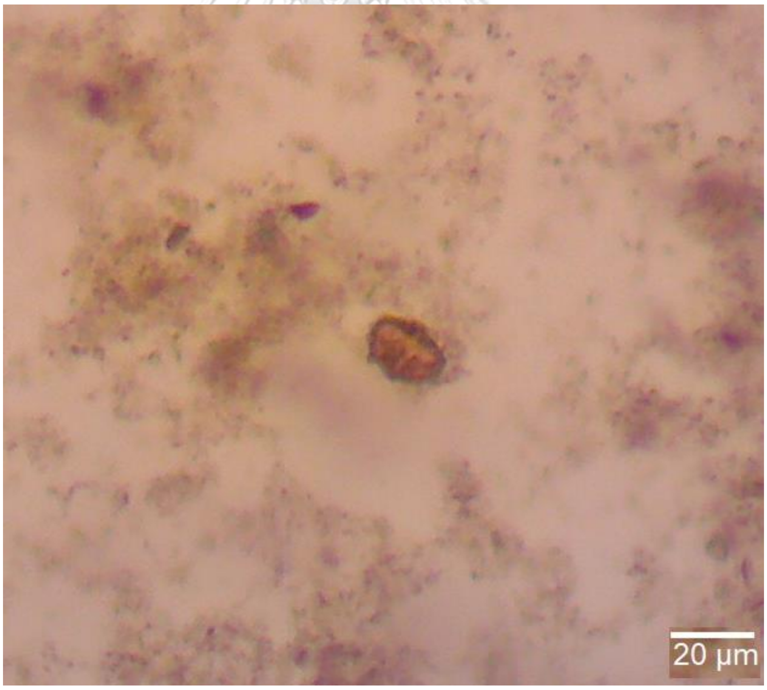

Figure 50 *Quercus*

VITA

NAME	Dissaya Sukaudom
DATE OF BIRTH	26 Nov 1996
PLACE OF BIRTH	Bangkok, Thailand
INSTITUTIONS ATTENDED	Mahidol University (B.Sc)
HOME ADDRESS	22/5 Moo 4 Kamnoet Nopphakhun, Bang Saphan, Prachuab khiri Khan 77140